

Indian Monsoon Cycles Through The Last Twelve Million Years

Shyam Murli Gupta

National Institute of Oceanography

Dona Paula-Goa, 403 004

Email: smgupta@nio.org

Abstract

It is an overview for general understanding of the nature, extent, causes and effects of the Indian monsoon cycles in the modern time and in the geological past. An attempt is made to present monsoon, an interdisciplinary subject, in simple ways by briefly introducing the atmospheric, oceanic, solar, planetary, and orbital forcing on monsoon, based on established phenomenon. It limits to encompass the statistically significant and reconstructed cyclic patterns in the Indian summer monsoon, primarily reported due to changes in the proxies for the Earth-Ocean-Atmosphere interactions (resulting into land-sea thermal contrast, inter tropical convection zone, winds, clouds, rains, El-Nino, sea surface temperature), solar (Sunspots, flares, and irradiance), lunar (tidal force), planetary (gravitational perturbations), and the Earth's orbital forces (the eccentricity, precession of equinoxes, axial tilt and orbital plane inclination), changing the amount of incoming solar radiation (insolation) during the last ~12 million years (Ma).

Key Words:

Introduction

In India, the word "Monsoon" is synonymous to "Mausam" which stands for the 4-months season of rain and wind accounting for ~90% rains from June to September, which is known as "Chaumasa" – starting with the plowing, sowing and harvesting of Kharif crop by the farmers. Another view is that, it originates from word "Mausim" used by Arab sailors for the southwest sea breeze from the Arabian Sea towards India. Meteorologically, monsoon is the seasonal southwest sea breeze that brings rains over India. Historical accounts narrate that generally monsoon sets in southern India in the first week of June ("आसाढस्य प्रथमदिवसे मेघमाल्लिष्टसानु" – Meghadutam, Kalidasa, ~434 A.D.), and within 4-6 weeks it spreads all over India. Monsoon played an important role in ancient India's prosperity ("Artha-Shastra", Kautilya, ~321-296 B.C). Prolonged droughts are believed to force agrarians of the Indus civilization to migrate elsewhere, and greener pastures of the Indian fields drew central Asians (Greek, Turks, Afghans, Arab, Persians, Mongols, French, Portuguese, British etc.) to invade, plunder, trade, and eventually settle in India during last ~500-2500 years B.P. Monsoon is also known for floods/drought causing agrarian economy to suffer, and its prediction based on certain trends in physical variables with predictive possibilities (Nicholls, 1983; Meehl, 1987; Hastenrath, 1987; Sadhuram, 1997; Gadgil *et al.*, 2002) are the most sought after, but the difficult task. A brief account on monsoon, its forcing mechanism, proxy indices, and its significant cycles in time scales of years, decades, centuries to thousand of years (ka) in the last ~12 million years (Ma) are summarized. Open access digital data of the published works on modern Indian Rainfall, Sunspot numbers and total solar irradiance (TSI), and solar insolation are analyzed afresh by the

Continuous Wavelet Transform and multi-taper method (MTM) for the spectral analyses, and the graphics are modified and designed in order to avoid copy right on published figures.

Indian Monsoon

Meteorologically monsoon is derived due to differential summer heating by the Sun's Incoming Solar Radiation (insolation) between the tropical Indian Ocean (causing evaporation, cloud formation and high atmospheric pressure with monsoonal SW winds), and the Asian landmass (causing extreme summer heat, low pressure and rainfall) due to atmospheric pressure and moisture difference. Thousands of years ago (ka) Indian astronomers accounted in the astronomical treatise "Surya-Siddhanta" (Burgess, 1860; Shukla, 1957; Thompson, 1997), that the Sun heats up the oceans from "Uttarayana" commencing on "Makar-Sankranti" when Sun is apparently over the tropics of Capricorn (Sishir Ritu, ~14th January) up till "Karka-Sankranti" with Sun over tropics of Cancer (Varsha Ritu, ~14th July), which results into rains over India, then Sun returns back ("Dakshinyana") towards tropics of Capricorn (Fig.1A).

The Sun is apparently over the equator twice in a year on ~21st March and ~21st September due to Earth's axial tilt (23.5°) resulting in equal length of the day and night (equinoxes), and thereafter moving towards summer and winter solstices on ~21st June (longest day) and ~21st December (longest night), respectively. Twice crossing over of equator by Sun heats up the tropical ocean, evaporates surface waters, makes clouds, which get transported by the monsoonal winds blowing towards India and resulting into rains. It is known as southwest Indian Summer Monsoon (ISM), and accounts for ~90% of total annual rain fall over India. A modern analog to above ancient description is the "Hadley cell" (Halley, 1686; Hadley, 1735), that brings moist air from oceans heated by the Sun, producing gigantic and towering clouds over enormous region south of equator (Fig. 1B). Moisture in the cloudy air condenses releasing latent heat and resulting in cold dry air at a height of ~15 km, spreading out over the tropic, and then descending at ~25-30° latitudes, which is the reason that most of the deserts are located between 20-30°. Dry air again returns towards equator, evaporating the sea, picking up the moisture on the way, making towers of clouds over the tropical ocean, and thereby completing Hadley cycle, which is widely accepted (Webster *et al.*, 1998).

Earth-Ocean-Atmosphere interaction

Physical and Topographic constrains:

Indian monsoon is bounded by the unique continental topography (Fig. 2A) that is characterized by the low lands in South-East Asia and Australia facilitating atmospheric interaction between the Western Pacific and Southern Indian Ocean trade wind (easterlies) domain unhindered. Trade winds during northern summer (May-July) are stronger than northern winter (Dec.-Feb.) in the southern Indian Ocean. While blowing east to west they encounter the high lands in Madagascar, East African and Arabian mountain ranges ($\geq 1-2$ km), which act as a physical barrier and turn them into monsoonal winds heading towards Indian subcontinent all along the Somalian and Arabian Margins in the Arabian Sea. The paleo-Tethyan mountain chain extending from Middle-East Asia, Hindukush, Himalaya, Tibet and Arakan-Yoma ranges ($> 3-5$ km) restrict the monsoon winds to cross over the Indian subcontinent and to reach central Asia. Consequently, most of monsoon rains are confined over the Indian subcontinent and Southeast Asia, and the central Asia is almost deprived of monsoon rains due to physical barrier of the paleo Tethyan Himalayan and Tibetan mountain chains. Winds blowing over Australian, African and Arabian deserts (Sirocco *et al.*,

1991) towards sea (Fig. 2A) add enormous dust (deMenocal, 2004) into wind-induced strong coastal and open-ocean upwelling system with high biological productivity during monsoon (Clemens, 1998).

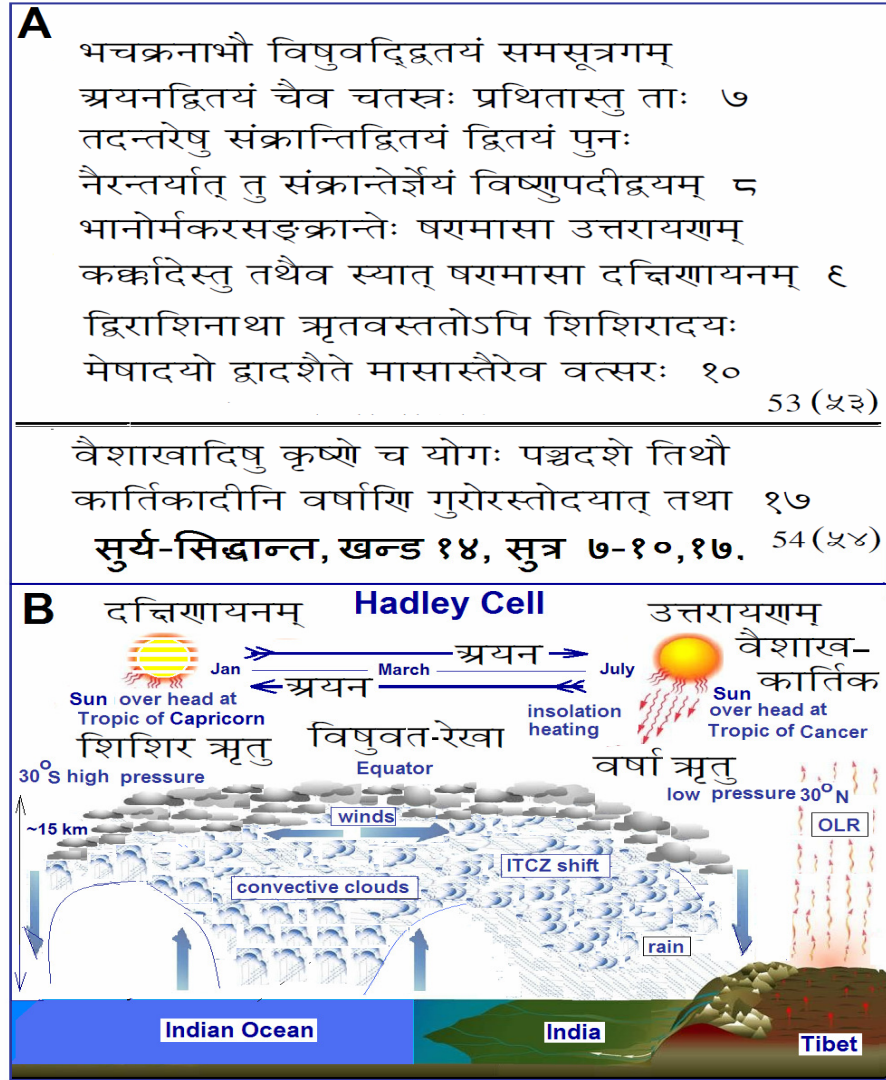


Fig.1.(A) Description of apparent crossing over of the Sun from tropics of Capricorn (December/January) across the equator in its northward movement (Uttarayana), en-route heating of the sea during summer, which results into rain when Sun is over head on the tropics of Cancer during Varsha-Ritu (June/July) as described in the "Surya-Siddhanta" (~400 years A.D.). (B) Somewhat analogous, what is described in (A), is the modern monsoon – a combination of Hadley-Cell, ITCZ, differential solar heating, pressure, outgoing long wave radiation (OLR) due to albedo effect from Tibet-Himalayan ice and forest cover, convective clouds, winds, and effect of all these parameters resulting into rains over the India. Sun during January is shown with white bands depicting its position during winter (Shisir Ritu), as the graphic is modified and designed for summer to emphasize the solar heating, convective clouds, winds, and the ITCZ position during July, when Sun's Uttarayana journey culminates at the tropic of Cancer resulting in torrential rains (Varsa-Ritu).

Inter-Tropical Convergence Zone:

Gadgil (1988) opined that monsoon, covering a wide geographic region in Afro-Asian region (Fig. 2B), is manifestation of atmospheric flow of moisture laden air causing equatorial cloudiness, which is termed as the Inter Tropical Convergence Zone (ITCZ) (Fig. 1B, Fig. 2B-D). Chen *et al.* (1988) found that Indian monsoon is characterized by annual cycle of divergent circulation of giant sea-breeze, and it is modulated by planetary-scale ~ 30 – 50 day low-frequency mode to establish an onset-active, break, and then revival-retreat of rains. This process is on round the year, and seasonal position of ITCZ boundary reflects seasonal shift (north/south of equator) with the Sun always overhead on it (Fig. 1A, Fig. 2B-D). ITCZ cloudiness is also more or less cyclic at ~ 30 – 50 days (Sikka and Gadgil, 1980), and pack of clouds get fragmented by varying wind speed during northward journey towards India, resulting in spells (7–10 days) of heavy showers with intermittent period of no rains, which gives enough time to farmers to plough, sow Kharif crop. Rain fall and prevalent winds during July (mid-monsoon, Fig. 2E) gives an idea on the extent of monsoon rains over Southeast Asia including Indian Ocean (<http://irid.ldeo.columbia.edu>). Indian monsoon often turns aperiodic and is a major hurdle in predictive meteorology. Empirical seasonal forecast of monsoon have moderate success for over 100 years, but modeling efforts have not been so successful in predicting monsoon accurately, as the simulation of mean structure of monsoon has been very elusive, and observed variability of relationships with forcing responsible has been often difficult to replicate (Webster *et al.*, 1998).

Tropical Warm Pools and Thermo-Haline Circulation:

Monsoon is affected by variations in numerous phenomenons in the Earth-Ocean-Atmosphere system. Some of them are (i) tropical Indo-Pacific reservoir of heat and salt as the warm pool (Fig. 2A-B), (ii) Indonesian through flow and the global thermohaline circulation by the conveyor belt distributing tropical heat and salt to polar regions (Fig. 2C), (iii) volcanic and cosmic dust/aerosols in atmosphere scattering away considerable amount of solar radiation and thereby cooling effect, (iv) atmospheric contents of greenhouse gases (CO_2 , CH_4 , NO_2 , CFCs, O_3) that absorb outgoing long-wave radiation (OLR) and heat up the atmosphere, (v) vapours and low lying clouds with a feedback mechanism (more the warmth, more water vapours absorbing more outgoing radiation), and (vi) ice and vegetation cover (albedo, ratio of reflected to incident radiation acting as another feedback mechanism). All these factors and their individual/cumulative effects are still not fully understood to the predictable extent, and so the monsoon often deceives millions to suffer.

India Meteorology Department (IMD) takes the Arabian Sea and southern Indian Ocean sea surface temperature (SST) during January-March which is correlated with rains ($r \sim 0.55$), as one of the input in forecasting Indian monsoon. Gadgil *et al.* (1984) found strong correlation with summer SSTs and cloudiness (rains). Besides, winter snow cover at Eurasian mountain causing albedo (ice reflecting radiation back to space), and east Pacific El-Nino-Southern-Oscillation (ENSO, Philander, 1983) effects, both are negatively correlated ($r = -0.46$) to Indian monsoon rains (Webster *et al.*, 1998). Monsoon is result of seasonal migration (Fig. 2B-D) of the ITCZ (Gadgil, 2003), and accumulation of clouds and rains due to southwest winds (Fig. 2E). Monsoon has large error ($\sim 15\%$) in forecast based 8–10 parameters significantly correlated with rains (Fig. 2B-C) used in predictive models. Besides, there are parameters like (i) Sunspots and radiation, (ii) Earth's orbital forcing and insolation, and (iii) planetary synod effect that are although known to affect climate on short scale, but their relationships with rains are yet to be established in empirical equations to be used in the predictive models of monsoon.

The ITCZ (Fig. 1B, Fig. 2B-D) and the tropical Indo-Pacific warm pool due to equatorial solar heating result in higher SSTs (Fig. 3A), which enhances evaporation at sea and supplies the vapors and clouds from ocean to atmosphere (Chao and Chen, 2001). Clark *et al.* (2000) found that SST during fall-winter before monsoon in tropical Indian Ocean correlates positively with subsequent monsoon rainfall, and they are negatively correlated with SSTs and the All India Rainfall Index (AIRI, Pathasarathy *et al.*, 1994) in the subsequent autumn in the northern Indian Ocean. They reported highest correlation (0.87) for the years following 1977 between the AIRI and the central Indian Ocean SST in the preceding September–November. These modern studies, one or the other way, directly or indirectly converge to ancient theme in Surya-Siddanta of warming of seas commencing from January through April-May, and resulting in rains during mid of Grisma to the end of Varsha Ritu from June-September. Monsoon rain water drains out into the Bay of Bengal and South China Sea resulting in lower salinity (<35 psu) in that region than non-monsoon regions (Fig. 3B) of the world oceans. Indo-Pacific tropical hot and less salty water leaks through passage between Antarctica and South Africa, becomes saltier due to en-route evaporation towards North Atlantic, and then get cooled due to lower SSTs at the Arctic circle, where it starts descending deep into water column to form a conveyor belt that returns through the deeper level back to the North Pacific along the Australia and New Zealand. Such re-distribution of heat and salt from the tropics to the pole has a great effect on regional and global climate including monsoon, and it is known as conveyor belt effect (Fig. 3C).

El-Nino and Southern Oscillation:

Besides, un-usual warming of eastern tropical Pacific Ocean known as El-Nino (Philander, 1983, Fig. 3D) also play role in the strength of the monsoon (Ashok *et al.*, 2001). El-Nino years are associated with poor monsoon (El-Nino 3+4 SST trend and monsoon rain correlation $r = -0.46$), while La-Nina eastern Pacific cooling events relate to good monsoon, which means good Kharif rice production. Variability in Indian rice production with time between 1960 and 1996 and the all-India rainfall index, the total summer rainfall over India, suggested that rice production has increased linearly (Gadgil, 1996). Webster *et al.* (1996) suggested that the years of deficit Indian rice production were associated with El-Nino years while rice abundant years were associated with La-Nina cold events in the eastern Pacific Ocean (Fig. 3 H). Strength and duration of the eastern Pacific warming due to the El-Nino and Southern Ocean Oscillation (ENSO), or cooling due to La-Nina, affects the domains and extents of the ocean, atmosphere, and tropical heat and salt reservoir – commonly known as the Indo-Pacific warm pool (Fig. 3A-B). El-Nino is somewhat predictable as the continuous wavelet transform (CWT) spectral analysis by method of Torrence and Compo (1998) reveals ~2.7-3.4- quasi-biennial oscillation (QBO), and ~11-years (Torrence and Webster, 1999) cycles in the modern time (Fig. 3E-d). There are several studies, which suggest that the ENSO phenomenon is cyclic in nature and its index is somewhat predictable. A sedimentary record of ENSO for the last ~2300 years in the form of lithological grey scale, Ti variation, and other productivity proxies from Peru Margin revealed highly significant ENSO cycles, mostly of solar origin, at ~250, 154, 83 (Gleissberg, 1958), 56–38, 31, 22–24 (cycles by reversal of magnetic polarity in Sun, Hale, 1924), ~11–9.4 (Sunspot), and typical ~7.4–5.7 years ENSO cycles (Agnihotri *et al.*, 2008, cf. fig. 8).

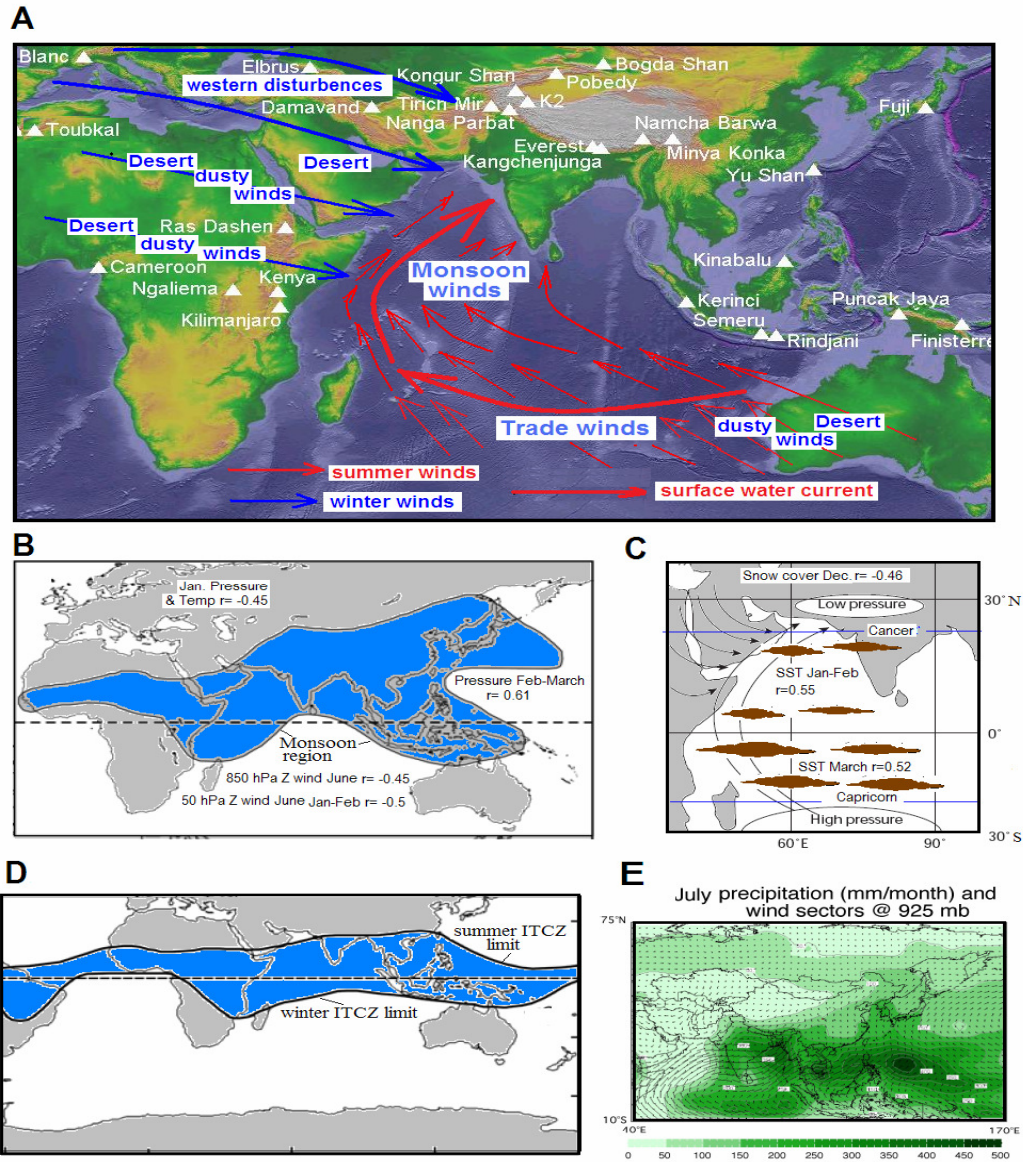


Fig. 2: (A) High mountains ($\geq 1-2$ km) of the Madagascar, East Africa, Arabia act as a orographic wall to divert trade winds blowing between Australia and Madagascar towards Indian subcontinent along African Margin over Arabian Sea, which culminates its northerly journey over India due to lofty mid-Asian high lands ($\geq 3-5$ km) including Himalaya and Tibet during monsoon season. Mountain peaks > 3 km are shown as triangle. Occasionally, low pressure over central Europe invades the monsoon systems as the western disturbances, and is shown as arrows from Mediterranean towards India across the lofty mountains in Afghanistan. Winter winds over African and Arabian and trade winds over Australian deserts bring eolian dust into Arabian Sea and central Indian Ocean (Clemens, 1998). (B) Monsoon regime over the Afro-Asian region. (C) Atmospheric circulation during Indian summer showing low pressure on India and high pressure in southern ocean, along with monsoonal wind directions from tropics of Capricorn and Cancer. (D) Seasonal changes in northern limit of the ITCZ. (E) Mean rainfall and winds averaged for July (<http://irid.ldeo.columbia.edu>). Correlation ($r =$) with monsoon rain and forcing parameters are depicted in B and C, which are used by IMD in monsoon forecasting.

Indian Rainfall:

All India homogenized mean rainfall data from 1871 (update on Parthasarathy *et al.*, 1994, IITM, Pune) has been extensively analyzed by various researchers suggesting better rainfall during La-Nina and drought like conditions during El-Nino events (Fig. 3F). The CWT spectral analysis suggests cycles at ~ 2.7 (similar to ENSO), 11-14 (Schwabe's Sunspot), and 80-years (Gleissberg, 1958) cycles (Fig. 3G-d). Spectral analysis (Schulz and Stattegger, 1997) of this data from 1871-2007 suggests cycles at ~ 54 , 17, 11, 7.5, 3.2, 2.7, 2.3 and 2 years (Fig. 3I). Harmonic analysis by Multi-Taper Method (MTM - Thompson, 1982; Ghil *et al.*, 2001; www.atmos.ucla.edu/tcd/ssa) as used in Gupta (2009), results in cycles at ~ 80 (Gleissberg), 22 (Hale), 7.5, 5.1, and 2.7 years (Fig. 4A), which are reconstructed and compared with rainfall time series (Figs. 4B-F). Varāha-Mihira (Brahatsamhitā, Ch. 8, v. 24-25) had accounted the ~ 3 , 5, 7, and 11 year rain cycles.

The 3-year rain cycle was attributed by Parāsara's saying "arka-varsa-nigraham" for influence of Venus on Sun induced rains, and it was associated with visibility of Venus in India. The 5-year rain cycle was described having 1st year of even rains (sama-vatsar), 2nd year early and good rains (pari-vatsar), 3rd year excessive rains (eda-vatsar), 4th year delayed rains (anu-vatsar), and 5th year deficient rains (id-vatsar), and ~ 7 , 18 (lunar eclipse) and 60 years (cross-product of 5 and 12 years Jupiter cycle) cycles in rains as per Iyengar (2009). Similar cycles are reported in the Sun's magnetic field at ~ 22 (Hale, 1924), 4-7 (ENSO) and 2-3 (QBO) cycles, and also in the historical US rainfall data (Rao and Hameed, 2003).

Indian Ocean Dipole:

Indian Ocean Dipole (IOD) is a quasi-periodic oscillation of SSTs between the positive, normal and negative phases of thermocline thickness (Saji *et al.*, 1999). A positive IOD phase having higher than average SSTs and higher rainfall in western Indian Ocean region, corresponds with cool waters in the eastern Indian Ocean - which results into droughts in Indonesia and Australia and vice versa during negative IOD phase. IOD is reported to affect strength of monsoon in India. On an average of 4 each positive/negative IOD events occur during every ~ 30 year (4×7.5) period with each event lasting ~ 6 months. It is worthy to note that El-Nino (Agnihotri *et al.*, 2008, cf. fig. 8b) and IOD-events both have cyclic changes at ~ 30 -31 years and ~ 7.5 years indicating influence of the Saturn's period.

Solar Variability and Monsoon

Agnihotri *et al.* (2002) found less intense Indian monsoon during periods of solar minima in the last millennium, and reported cycles at $\sim 200 \pm 20$, 105 ± 15 and 60 ± 10 years. The 60-yr cycle observed in the instrumental rainfall data appears to be of solar origin and supports the hypothesis of solar control on the Indian monsoon on a multi-decadal time scale. Agnihotri and Dutta (2003) suggested that century scale monsoon rain fall patterns in the Indian and Chinese rain is due to manifestation of solar changes by relating them to variability in Sun's radiation. Kodera (2004) studied Sun's influence on monsoon and found that it originates from the stratosphere through modulation within the equatorial troposphere, and produces a north-south seesaw of convective activity during summer over the Indian Ocean. Higher precipitation over southeast Asia and India are reported to occur

during high solar activity. Therefore, variability in solar activity and its effect on Indian monsoon are presented below.

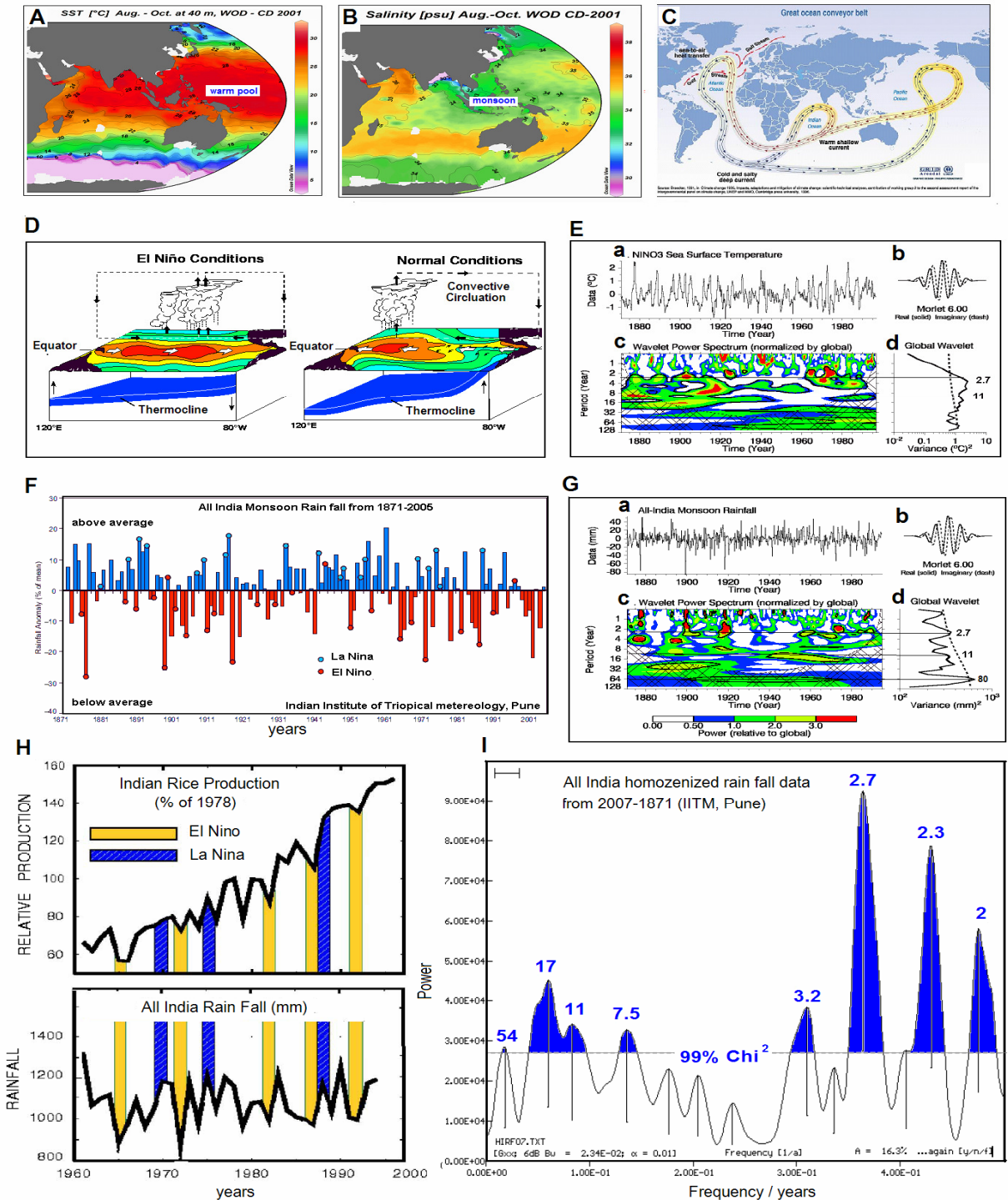


Fig.3: (A) SST isotherms in the Indo-Pacific Ocean showing tropical warm pool and (B) surface salinity showing less saltier water in the Bay of Bengal and South China Sea due to monsoonal (Aug.-Oct.) fresh water flux from the Indian and Chinese rivers, respectively (WOD-CD-2001,ODV packag- Schlitzer, 2001). (C) Global thermohaline conveyor belt path distributing the tropical heat and salt to the north Atlantic and

then reverting back to North Pacific Ocean (<http://irid.ldeo.columbia.edu>). (D) El-Nino and normal tropical Pacific Ocean conditions showing changes in position of convective circulation, thermocline depth and isotherms. (E) CWT spectral analysis of Nino-3 data showing 2.7 and 11-16 years cycle (Torrence and Webster, 1999). (F) Indian monsoon rainfall relative anomaly data from 1871-2005 (IITM, Pune) showing correspondence with drought and El-Nino, and good rains with La-Nina years. (G) CWT spectral analysis of Indian rainfall anomaly (Torrence and Compo, 1998) shows 2.7 (QBO), 11 (Schwab) and 80 (Gleissberg) years cycles. (H) Relative rice production compared to 1978 base year with upward trend due to green revolution, and All India Rain Fall during El-Nino and La-Nina years from 1960-1996 (Webster *et al.*, 1998). (I) Spectral analysis of All Indian Rain Fall from 1871-2007 showing cycles at ~54, 17, 11, 7.5, 3.2, 2.7, 2.3 and 2 years.

Variability in Sun's diameter:

At present Sun's diameter is ~1 million miles (MM), and yearly small changes in it are generally not noticeable. With advent of research satellites, our understanding on Sun, Earth, Moon and other planets witnessed a phenomenal change. King (1973) reported that Sun's radius and its luminosity (solar constant) is not the same over the time. Eddy (1977), Eddy and Boornazian (1979) opined that Sun's radius is reducing at the rate of ~0.1%/century (~4 feet/hour). Eddy *et al.* (1982) reported ~0.05% change in Sun's diameter from 1863-1953 affecting its luminosity, which noticeably affected Earth's climate. Gilliland (1981) suggested large changes in Sun's luminosity during the last 265 years due changes in its radius, while Sofia *et al.* (1983) analyzed duration of total solar eclipses from 1925 to 1979 records, and found that during 1925 Sun's radius was ~375 km larger than at 1979. Sun's radiation changes due to variation in its diameter and its magnetic field, affect amount of the Total Solar Irradiance (TSI) received at the surface of Earth. Variability of TSI depends on changes in Sun's diameter, heat transport through the convective and radiative zone, temperature of photosphere, amount of magnetic flux on the Sun's surface, which is the perturbation in Sun's magnetic flux due to Sunspots, solar flares and prominent eruptions also known as solar tsunami (Fig. 5A). Cosmic solar rays produce cosmogenic ¹⁰Be in the atmosphere due to spallation of nitrogen and oxygen atoms, while ¹⁴C is formed in the atmosphere by the interaction of cosmic ray produced neutrons with nitrogen nuclei (Stuiver and Quay, 1980), and both are very good proxies for solar activity. Based on relationship between TSI and solar magnetic field, obtained from the cosmogenic radionuclide ¹⁰Be measured in ice cores, TSI is reconstructed in the past. Reconstruction of TSI is based on quantitative estimate of changes in ¹⁴C and ¹⁰Be cosmogenic radionuclid production rates (Bard *et al.*, 2000; Bond *et al.*, 2001). Reconstruction of TSI for the last 9300 years by cosmogenic radionuclide ¹⁰Be measured in ice cores was done by Steinhilber *et al.* (2009), who reported increase in TSI solar-cycles averaged from the Maunder Minimum to the present amounting to 0.9 (± 0.4) Wm⁻². Multi-taper method (MTM) based spectral analysis of TSI time series of Steinhilber (*et al.*, 2009) revealed Suess, Gleissberg and several other cycles (Fig. 7A), similar to those found in reconstructed Sunspot numbers of Solanki *et al.* (2004) as shown in Fig.7 (B-I). Chakraborty and Bondyopadhyay (1986) described effect of changes in solar variability influencing rainfall pattern, Chowdhury *et al.* (1981) considered it as a potential factor for droughts in India, whereas, Reid (1987) described the influence of Sun's radiation changes on global SSTs and its potentials in weather changes.

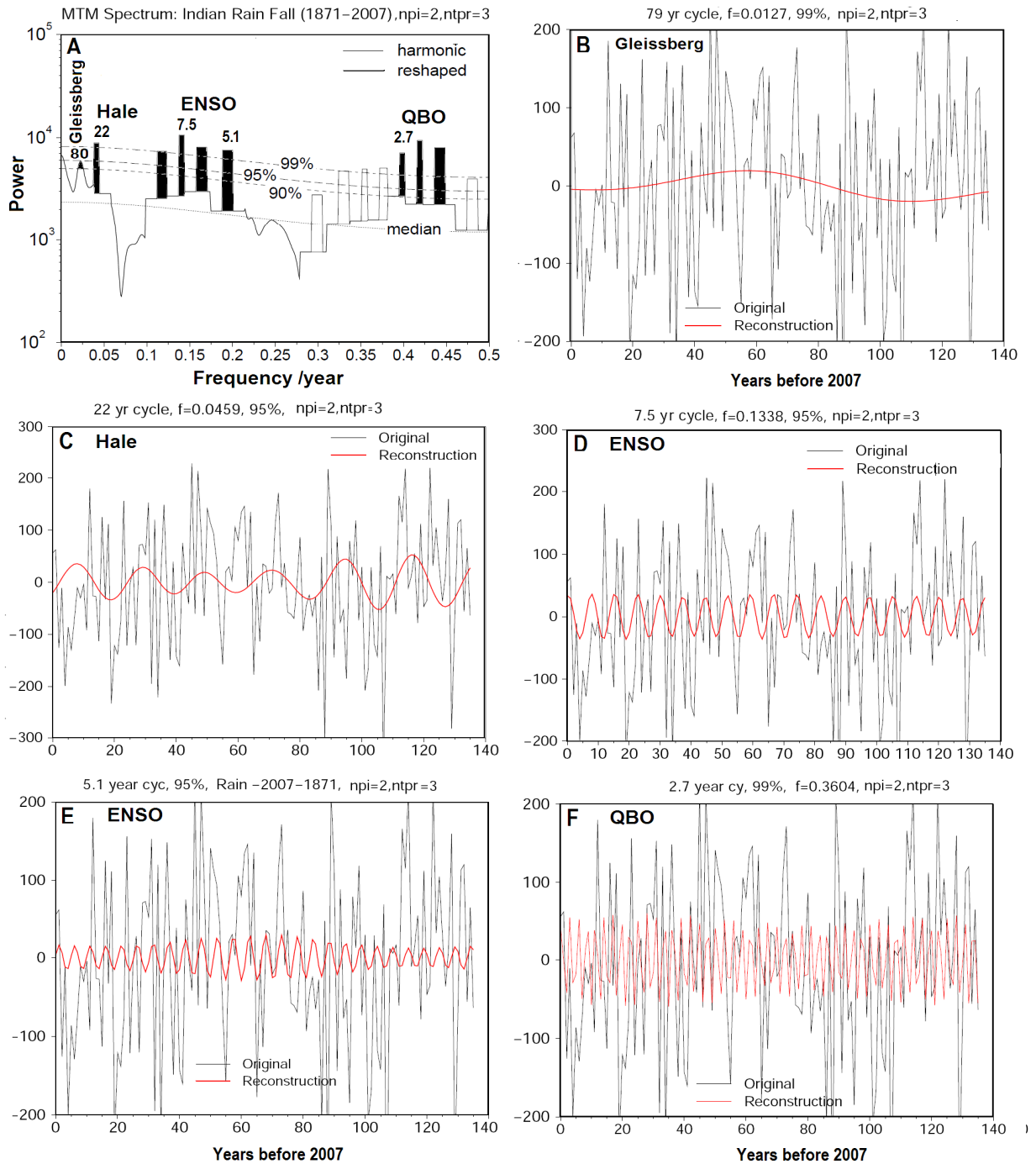


Fig. 4: MTM harmonic analysis of All India homogenized rainfall data (IITM, Pune) from 2007-1871 (A) along with reconstructions of significant cyclic trends at ~79- (B, Gleissberg cycle), 22- (C, Hale), 7 and 5 (D-E, ENSO), and 2.7 year (F, quasi-biennial oscillation) cycles.

Sunspots and changes in Sun's magnetic field:

Hale (1924) demonstrated that the magnetic polarity in southern solar hemisphere Sunspot groups is the opposite to that in the northern solar hemisphere. Nicholson (1937) reported that at the end of each 11-year Sunspot cycle of rising and falling numbers, the polarity of spot group reverses, and at the end of 22 years, Sunspot polarities on both hemispheres of the Sun had alternated through one complete full wave of positive and negative polarity. The Sun's surface is highly dynamic with a variability of 11-year solar activity cycle in Sunspots (+ flares and eruptive prominence). During a solar active maximum, number of Sunspots increase on the surface on the Sun. Sunspots (Fig. 5A, a-b) are relatively cooler (umbra, $\sim 4000^{\circ}\text{C}$, $4\text{-k}^{\circ}\text{C}$) areas of $\sim 100,000$ km in diameter encircled by warmer regions (penumbra, $\sim 5\text{-k}^{\circ}\text{C}$) on Sun's surface ($\sim 6\text{-k}^{\circ}\text{C}$), and hence appear as black spots (Hoyt, 1979). Solar flares/tsunamis are caused by coronal mass ejection consisting of the geomagnetic storm of super-hot gases and charged particles travelling at speeds of ~ 1 million miles/hour thrown out into the space. Usually, the deeper explosions within Sunspots are the areas from where solar flares erupt out into space. The last solar maximum was in 2001 (Fig. 5A-c), and next is awaited in 2012.

Heat received by the Earth from the Sun's radiation is affected by number of Sunspots, solar flares and TSI (Fig. 5 A, a-c). Variation in solar flares (Fig. 5A) with time suggested flares cycles at $\sim 9\text{-}11\text{-}$, ~ 2.25 years, and 3 months with potential in forecasts due to being in phases in the Sun's motion around the center of mass of solar system, and with a cyclic pattern in change in angular acceleration of tidal forces exerted by planets Venus, Earth, and Jupiter (Wood, 1972; Okal and Anderson, 1975) and other planets (Landscheidt, 1984) (Fig. 5F). The TSI is value of solar energy flux, over an area of 1 m^2 oriented towards the Sun, which arrives at top of Earth atmosphere (Fig. 5A,d) at a distance of 1 astronomical unit (AU, mean distance from Sun to Earth). The TSI, Sunspot, solar flare, and magnetic flux of charged particles/radio-flux are more or less synoptic in nature (Fig. 5B). Noisy daily, monthly and yearly Sunspots data, once smoothed with mean values, derives the predictive trends (Fig. 5C-D). A comparison between annual mean Sunspots as an index of solar activity (changes in magnetic field, diameter, and solar flares), and homogenized All India rainfall data from 1871-2007 (IITM, Pune) revealed a very good visual correspondence between the two time series (Fig. 5, E). Bell (1977) observed that the August (monsoon) sea level pressure over India flipped off from positive to negative sign with annual Sunspot numbers at ~ 1910 , in contrast to the close correspondence in the late 1940s. The switch over in their relationship at $\sim 1920\text{-}25$ was marked by a change from zonal to meridional circulations at the mid-latitudes ($\sim 30^{\circ}$), which reflected the reversal of Sun's polarity 22-year Hale cycle. Hiremath (2006) studied correlation coefficients for January–February, March–May, June–September and October–December and, annual mean data of Sunspots in different Sunspots cycles over last 130 years, and found that Indian rainfall is correlated with Sunspot activity with a trend of higher rainfall during low Sunspot activity. He suggested a possible physical connection between Indian rainfall and Sunspot activities and flux of cosmic rays. Sunspot activity affects annual mean temperature over India (Joseph and Amatya, 1986), which modulates landmass heating affecting the monsoon. These results concur with Sen Gupta (1957), who reported Sunspot cycles in regional rain-fall and suggested that it negatively affects Indian monsoon system, i.e., more Sunspots result in failure of the monsoon rains.

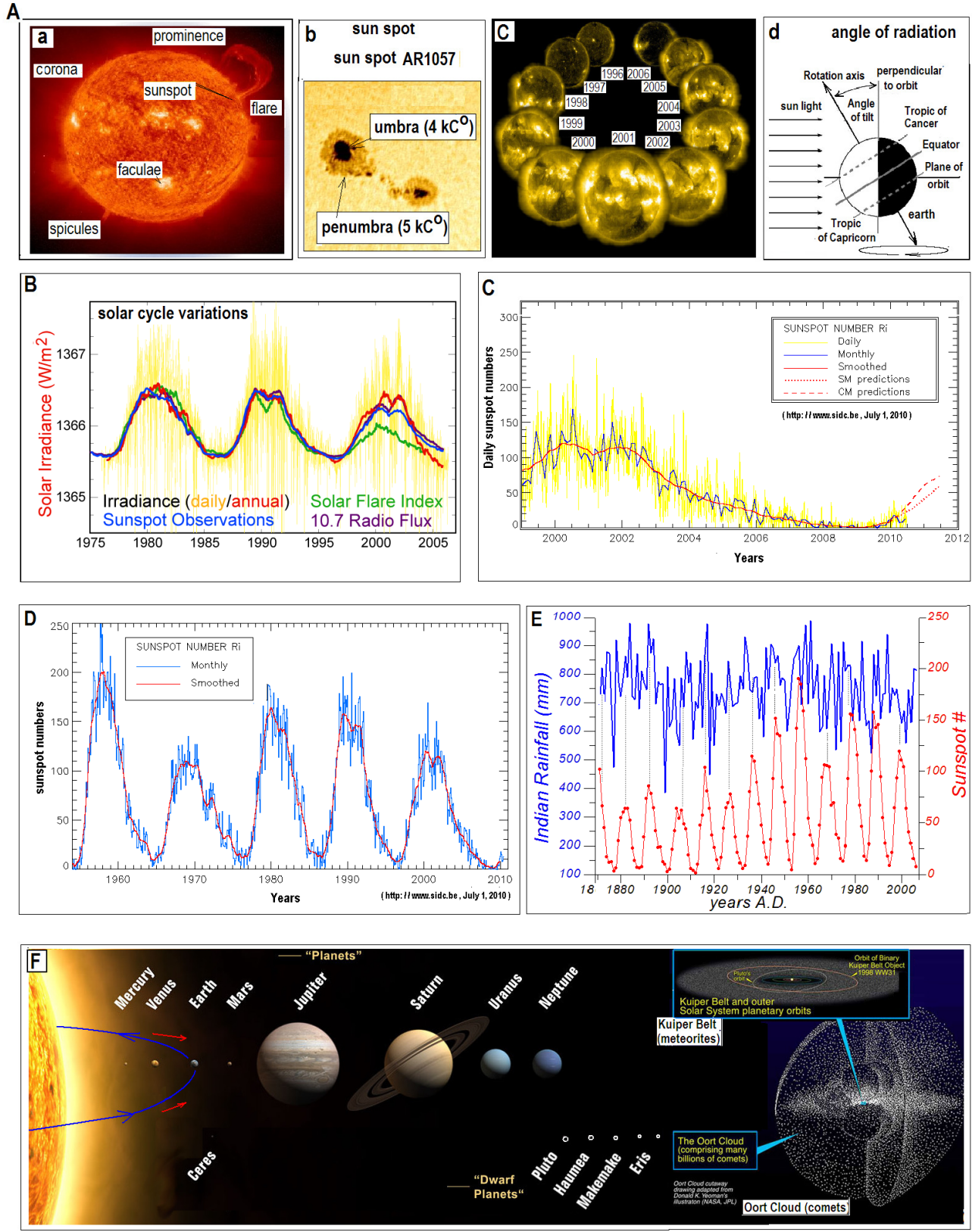


Fig. 5: (A) Surface of the Sun with corona and photosphere showing Sunspots, faculae, spicules, flares, and prominence (a), a typical Sunspot with umbra and penumbra (b), last Sunspot cycle from 1996-2006, with activity maximum at 2001 (c) and angle of radiation received at Earth over the tropics and poles (d). (B) Synoptic variation in solar irradiance, Sunspots, solar flares, and radio flux from 1875-2005 showing similar origin. (C) Daily and monthly smoothed Sunspots and their predictable trends. (D) Monthly Sunspots raw and smoothed data from 1950-2009. (E) Correspondence between All India Rainfall from 1871-2007 (IITM, Pune) and numbers of Sunspots. (F) Edge of solar system showing a hypothetical conjunction of all the planets in one side of the Sun. Arrows from the Earth's orbit towards the planets depict forward drag (backward pull) effect of conjoined planets on Earth's speed due to synod phenomenon that increases/decreases the length of summer/winter depending on the season of conjunction event. Also shown are the Kuiper meteoritic belt and Oort clouds of comets that occasionally de-established due to galactic tides (Napier, 2001, 2006) and enters in solar system as distant visitors along with meteoritic showers and cometary-dust. Graphics in A-D and F are from www.wikipedia.com.

Sunspot cycles in Monsoon:

MTM harmonic analysis of Sunspot numbers (www.sidc.be) for the 257 years (1750-2007) revealed cycles at ~ 111 years, 28.5 and 17.5 years lunar tidal cycles, 9-11 (Schwabe), 4.5-7 years sub-decadal, and 3-2.5 years QBO cycles (Fig. 6A). Although, the 111 year cycle is 90% significant, it could very well be considered as a long term trend than a predictable cycle, but the century scale variability in paleo-climate data often reported. A conspicuous increase in long term trend from 0-70 to years in the time series (Fig. 6B) is analogous to global warming (GW) trend, and raises concern that GW could also be due to manifestation of increased Sunspot activity in the last 70 years. The 28.5 year cycle (Fig. 6C) is very close to Saturn's orbital period (29.45 years) around the Sun suggesting that it could be due to increase in Sunspot activity by the gravitational perturbation of Saturn. The ~ 17 year harmonic (Fig. 6D) is close to Soli-Lunar cycle of ~ 18 years, which is widely reported in tidal forcing of Sun-Moon-Earth system, and suggest that analogous to Earth's tide effect, Moon might be having similar effect on Sun, or more because Sun is gaseous (more fluid than Earth) in nature. The ~ 11 and 9 year are well known Schwab cycles. Amplitude of ~ 11 year cycle has remarkable increased since last 80 years suggesting that global warming could possibly be due to natural variability in the Sun (Fig. 6E-F). The ~ 7 year (Fig. 6G) and ~ 5 -5.6 cycles (Fig. 6H-I) suggest intra-decadal variability recorded in several times series, whereas 4.7-3 years cycles (Fig. 6, J-L) are represented in ENSO variability and Indian (IITM, Pune), Chinese and US rain fall data (Rao and Hameed, 2003), and Antarctic ice core (Naik *et al.*, 2010). Besides, these individual cycles also produce larger cycles either by the way of amplitudes modulation or being in resonance with two are more closer cycles - for example pairs of (i) ~ 2.7 and 3 year cycles and (ii) ~ 4.7 and 5 and 5.5 years cycles as shown in Fig. 6, and they are shown as incomplete curved envelopes as being indicative of the amplitude modulated higher cycles. The ~ 22 - (Hale), 90- (Gleissberg, 1965; Feynman and Fougere, 1984), 208- (Suess), and 2300-year (Hallstatt) Sunspot cycles are reported from flood plain, lake, and varved sediments (Hameed *et al.*, 1983). Varved sediments deposited by Indus River off Karachi are reported to exhibit cycles ~ 125 , 29.5, 18.7, and 12 years (von Rod *et al.* 2006, cf. fig. 11). Time series analysis of the magnetic susceptibility in a sediment core (SK 148/55) located off Ratnagiri (east Arabian Sea), resulted in precipitation cycles at ~ 2200 , 1350, 950, 750, 470, 320, 220, 156, 126, 113, 104 and 92-years during the Holocene (Thamban *et al.*, 2007). Recently, Scafetta (2010) analyzed several global surface temperature records since 1850 and found

that the records deduced from the orbits of the planets present very similar power in the spectral results. The large climate oscillations with peak-to-trough amplitude of about 0.1°C and 0.25°C, and periods of about 20 and 60 years, respectively, are reported to synchronize with the orbital periods of Jupiter and Saturn, while Schwabe and Hale solar cycles, and 9.1-year cycle synchronized to the Moon's orbital cycles are reported in these temperature records.

Sunspot in the past:

Depending on Sunspot numbers and cosmogenic nuclides ¹⁴C and ¹⁰Be, periods of low solar activity called as Oort minimum (980-1120 A.D.), Wolf minimum (1282-1342 A.D.), Spörer minimum (1416-1534 A.D.), Maunder minimum (1645-1715 A.D.) and Dalton minimum (1790-1820 A.D.) are reported to affect the monsoon strength. Solanki *et al.* (2004) reconstructed Sunspot number by dendrochronologically dated ¹⁴C content in wood, which were positively correlated with solar irradiance in the last ~11400 years.

MTM harmonic analysis (Fig. 7B) of paleo-Sunspots data of Solanki *et al.* (2004) revealed significant cycles at ~192 (Suess), 89 (Gleissberg), 60 (2 X 30 year Saturn's period), and 42 years cycles, which correspond to planetary orbital periods of Neptune, Uranus, Saturn (Fig. 5F), respectively. All significant cyclic components in paleo-Sunspot data are reconstructed and compared with original time series, which invariably suggested changes in the amplitudes between ~4000-8000 B.P. (Fig. 7, C-I), that coincides with "Holocene Optimum" - a period of stronger monsoon than present.

Foraminiferal variation of *G. bulloides* species in a sediment core revealed a ~2200 years cycle in monsoonal upwelling record from Arabian Sea (Naidu and Malmgren, 1995), which could possibly be bundle of (200 X 11) Schwab cycles. Gupta *et al.* (2005) studied variation in monsoon upwelling index *G. bulloides* percentage in Hole 723A from the Oman Margin for the last 12-ka and compared it with Sunspot numbers (Solanki *et al.* 2004) and North Atlantic Hematite percentages. They reported monsoon cycles at ~1550, 152, 137, 114, 101, 89, 83, and 79 years and compared them with Sun-spot cycles. Monsoon variation in the form of thickness in varved sediment derived from Indus river off Karachi with high resolution record for the last 5-ka, revealed variation in Indus river sediment cyclically at ~1470 (Bond cycle), and 280, 200, 125, 95, 56, 39, 30, 26, 23, 19, 14 and 12 years, due to multiples of basic ~4.4 and 9.3 years Moon's tidal cycles (von Rad *et al.*, 2006). Indian rainfall, Sunspot, TSI, El-Nino, and Indus derived varved marine sediments, all show common cycles of ~11-12 and 2.7 years and are attributed to solar radiation variability. Alternatively, these cycles could also be due to the modern micro-variations in the precession, tilt and eccentricity of the Earth's orbit. Bertrand *et al.* (2002) did multi-taper spectral analyses of the eccentricity, tilt and precession values for the last 1-ka after de-trending them, and reported similar ~11.9, 5.9, and 2.7 years cycles present in eccentricity and precession, which they attributed due to gravitational perturbation of Jupiter, its 2nd harmonic, and Venus - Earth (Ve - 2E), respectively. Jupiter completes its journey around the Sun in ~12 years, and according to Indian saying - "□□□□ □□□□, □□□□ □□□□□ - □□□□ □□□□□, □□□□ □□□□" - every 12th year just after flowering of bamboos the crops fail due to scanty rains. Currie and Fairbanks (1985) reported drought/floods at ~18 lunar tidal and 11 Sunspot cycles in the Chinese rains emphasizing its global implications.

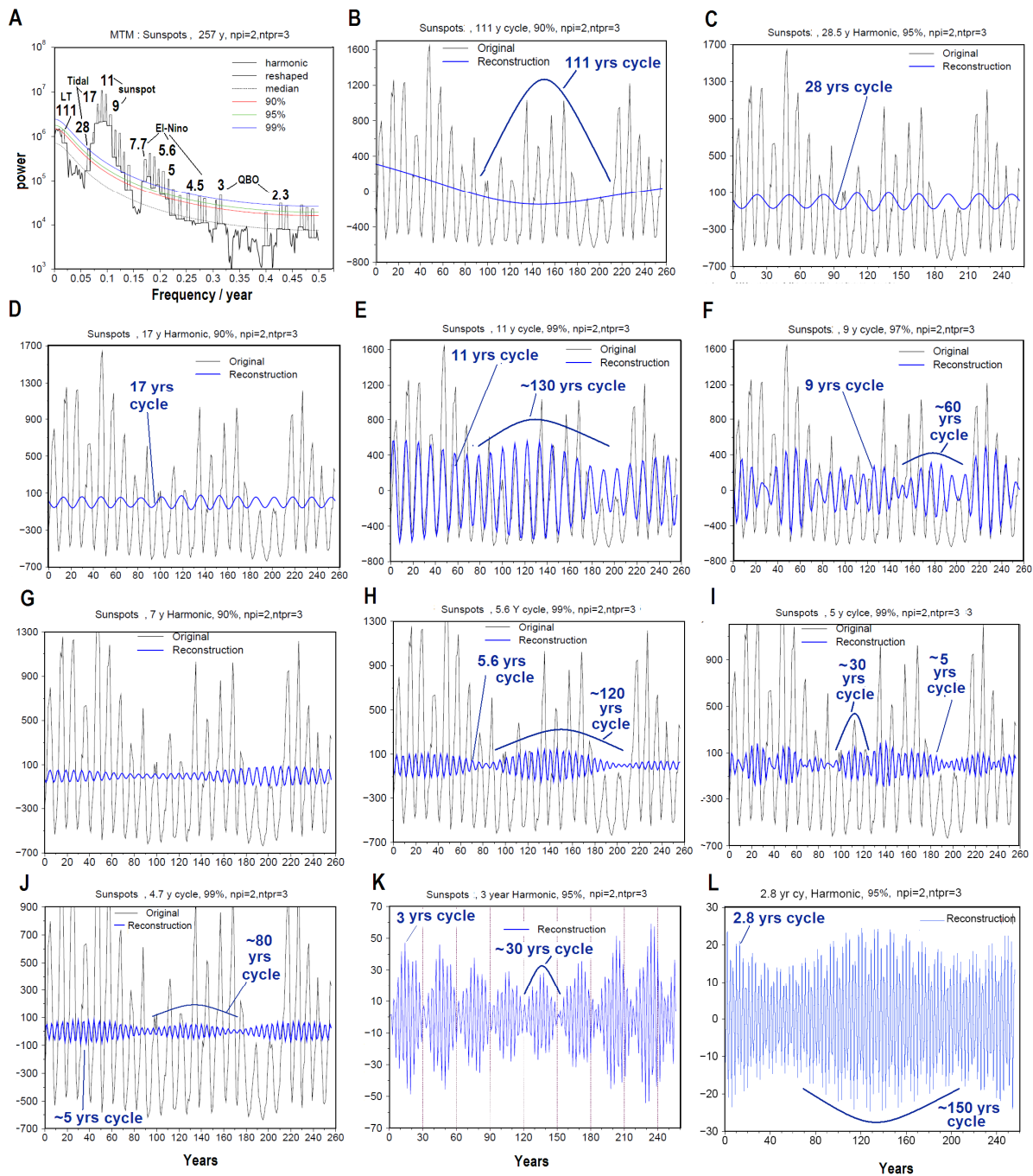


Fig. 6: MTM harmonic spectral analysis (A) of Sunspot data for last 257 years (courtesy: www.sidc.be) showing cycles at ~111- (B), 28.5- (C), 17 (D), 11- (E), 9- (F), 7- (G), 5.6- (H), 5- (I), 4.5- (J), 3- (K) and 8-years (L) cycles. Smaller cycles also produce larger cycles by amplitude modulations, shown as incomplete curved envelopes of large cycles at 30, 60, 80, 120, 130, 150 years.

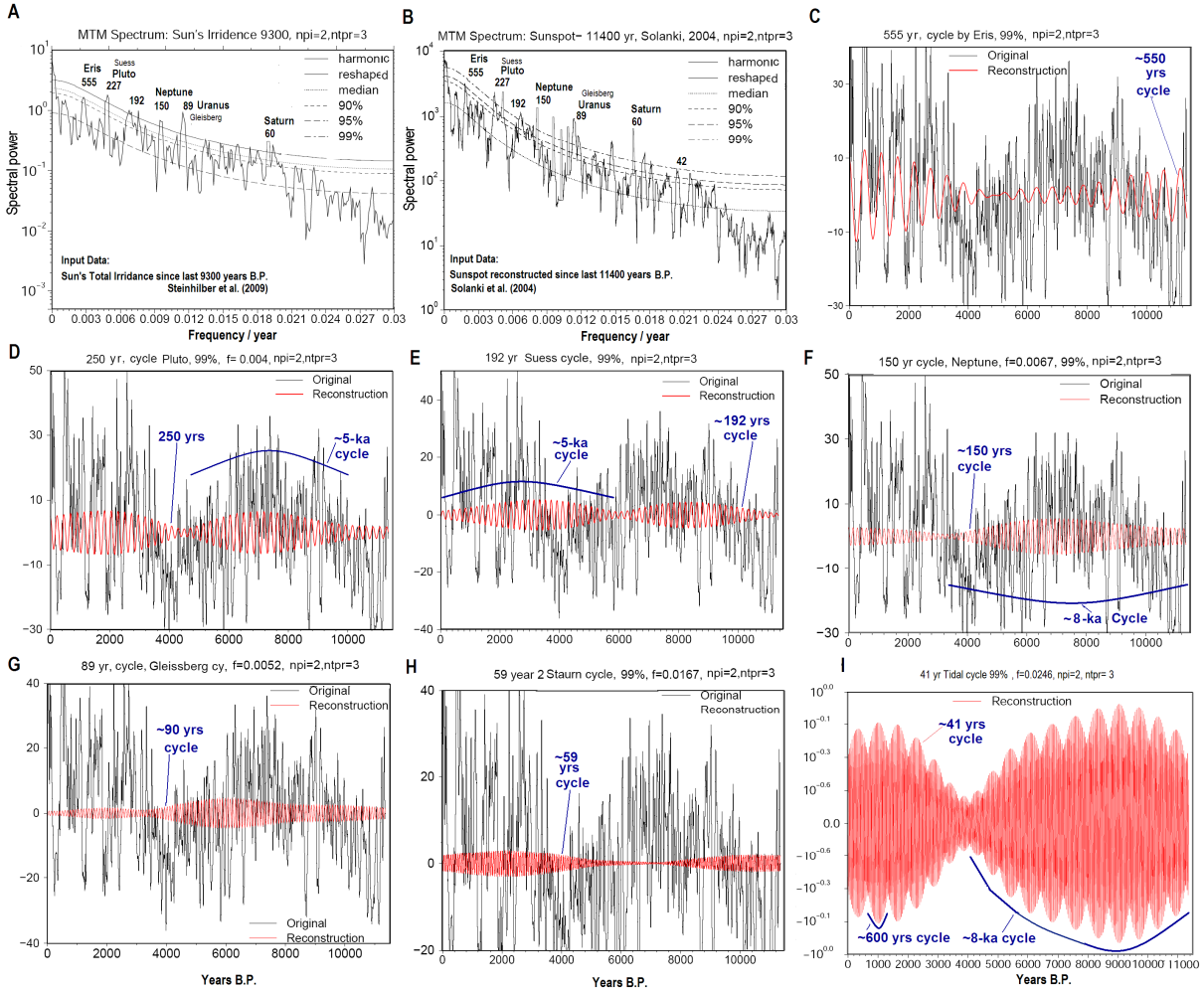


Fig. 7 : (A) MTM harmonic analysis of reconstructed TSI (Steinhilber *et al.*, 2009) for last 9.3-ka and (B) Sunspot numbers (Solanki *et al.*, 2004) for last 11.4-ka showing significant cycles at ~555 (C, Eris), 250 (D, Pluto), 192 (E, Suess), 150 (F, Neptune), 89 (G, Uranus/Gleissberg), 60 (H, 2x30 period of Saturn) and 42 (I, tidal) years cycles. Gleissberg cycle reconstructed and compared with Sunspot numbers suggesting that cycle was more pronounced during Holocene Optimum (>4-11-ka) with stronger monsoon than in last ~4-ka (G). Smaller cycles produce larger cycles by amplitude modulation shown as incomplete envelopes of larger cycles at ~600-, 5000-, and 8000 years.

Synod effect on Earth:

The gravitational pull/push of the planets like Venus, Mars, Jupiter, Saturn, Neptune, and the Trans Neptune Objects (TNO's) alters normal speed of Earth on its way around the Sun. Although, the time taken by Earth to encircle the Sun remains the same (365.25 days), Earth speeds up when it is under influence of gravitational pull of giant planets lined up in a group (within 30°) with Sun (conjunction/ synod), but when Earth travels away from them, its speed is reduced (Fig. 5F). Result is that the Earth takes less time to travel half of its journey, when it is closer to the conjunction of giant planets due to acceleration by pull effect of gravitational force of conjoined planets, whereas it spends more time in next half of

journey on far side of planets conjoined with Sun. If the conjunction happens in summer half of the year and Earth is moving farther to Sun, travel time increases due to pulling backward effect resulting in few days longer summer and vice versa. For example, in January 1665 giant planets were conjoined with Sun within 45° to Earth, which resulted in increased winter, and shortening of summer by 2 days resulting in $\sim 1\%$ change in seasonal heating by Sun (Burroughs, 2003). The Monsoon prolonged ~ 5 weeks when Sun, Venus, Mercury, Mars, and Saturn are within 60° in tug of war (180°) with Jupiter in 2010 causing unprecedented rains and floods. Outer planets Jupiter, Saturn, Uranus, Neptune, and TNO bodies like Pluto, Eris and Sedna on an average take $\sim 11.87, 29.45, 84.07, 165, 248, 557, 1250$ years to go around the Sun in their orbits, respectively (en.wikipedia.org/wiki/Orbital_period). These planetary periods nearly coincides with Indian monsoon record cycles at $\sim 11, 30$ (Neff *et al.*, 2001), 90 (von Rod *et al.*, 1999) and 180-200 years (Tiwari *et al.*, 2006), 245 (von Rod *et al.*, 1999), 584 (Hong *et al.*, 2001), 1100 (Neff *et al.*, 2001; Leuchner and Sirocko, 2003), and 2200 years (2^{nd} harmonic of 1100 years in Arabian Sea upwelling index, Naidu and Malmgren, 1995) monsoon cycles mainly due to reported Sunspot activity. Nigam *et al.* (1995) reported rain-proxy foraminifers changing at the Gleissberg cycle (80 ± 10 years). Similarly, the Chinese rain records are reported to have cyclic variations at $\sim 70, 80, 90, 107, 110, 123, 134, 141, 162, 198, 205, 249, 278, 324, 389, 467, 584, 834$ and 1060 years (Hong *et al.*, 2001). The gravitational perturbation of planets affect in similar way in Sunspot dynamics (gaseous star) as it affects the monsoon on Earth, or vice versa. Even in modern time when changes in Earth's orbital eccentricity, precession and tilt are minimal and un-noticeable, their micro variations may be altering the monsoon at shorter biennial to decadal cycles. Such an argument is based on the MTM spectral analyses of eccentricity, tilt and precession values from 2000 to 1000 A.D, which revealed yearly and decadal cycles both due to eccentricity and precession at ~ 11.9 (originating by period of Jupiter), 5.9- ($1/2$ of Jupiter's period), 4- and 2.7- (both beat of Venus and Earth), and due to axial tilt at ~ 18.6 (due to Moon's orbital change) attributed to orbital/gravitational forces of Jupiter and other planets (Bertrand *et al.*, 2002).

Sun-Moon tidal effect

Earth orbits around the Sun and the Moon orbits around the Earth. Both have elliptical path, and inclinations in their orbital planes (ecliptics) makes a complex orbital dynamics of tidal forcing due to gravitational pull of the Sun and Moon on the Earth. Earth's rotation and Moon's orbital motion around it exerts high and low tidal stress twice daily on ocean (also in atmosphere). As Moon completes its orbit around Earth every 27.5 days, it takes 13 rounds (lunar tidal months) of Earth to accompany it around the Sun in a year, and it is basis of India's lunar calendar with provision of an "adhi-masa" and 12 lunar months. Besides, monthly lunar cycles of ~ 28 days, Earth-Moon-Sun system also generates two other main cycles of 8.9 years (due to advance of longitude of Moon's perigee), and 18.6 years (due to regression of the longitude of the node), in addition to $\sim 13.6, 27.2$ and 42 years tidal cycles of very complicated orbital dynamics of Earth-Sun-Moon system. All these tidal cycles ($\sim 8.9, 13.6, 18.6, 27.2, 42, 179$ years) and their multiples are found in the Chinese paleo rainfall data (Currie and Fairbank, 1985). Keeling and Whorf (2000) found close similarity in mean of ~ 180 -year tidal cycle ($1/10$ of the 1800 year cycle) and the 179.2 years cycle of the Sun's rotation around the center of mass of the solar system as a manifestation of planetary resonances, and reported that 90-year cycle may vary from 84 to 93 years, and its modulation produces a large cycle of ~ 5000 years. It is interesting that $\sim 18, 90-95, 180, 1470, 1800,$ and 5000 years cycles are reported in monsoon records from stalagmites and wind strength preserved in sediments off Oman and Karachi (von Rod *et al.*, 2006). Although, Sunspot activity is within the Sun, its manifestation by gravitational

and tidal forcing of planets is vital for climate changes. Sun-Moon gravitational perturbation affects Earth's axis to precess (move backward) on its orbit at the rate of 51"/year, which alters equinox-precession from ~25- to 23-ka cycle. Surya-Siddanta described precession of the Earth thousands years ago (Jha, V. jyotirvidya.wetpaint.com/page/Ayanamsha+vs+Precession, Hari, 1997).

Orbital Forcing on Monsoon

Changes in the Earth's orbital eccentricity (e), precession of equinoxes (p), axial tilt (t), and inclination (i) of orbital plane (relative to invariable plane of Sun and Jupiter) affect the climate including monsoon significantly. Orbital variables are summarized for the last 3-Ma along with MTM results with significant cycles (Fig. 8).

Earth's orbital eccentricity:

Earth's orbit around the Sun is relatively circular at present (0.017), affecting ~6.7% change in the Sun's radiation reaching at the Earth's surface, but it was highly elliptical (0.06) in the past (Fig. 8A-a, D). Cyclic variation in shape of orbit from nearly circle (e = 0.0) to ellipse (e = 0.06) at every ~100- and 400-ka (Fig. 8A-a, D-E) is called eccentricity [$e = (a-p)/(a+p)$, a= aphelion and p=perihelion distances of the Earth from Sun in the orbit, perihelion: Sun closest to the Earth, 146.1 million km; aphelion: Sun farthest away, 151.1 million km] (Berger, 1977). It changes due to variations in gravitational pull/push (perturbation) on Earth's orbit by other planets like Venus, Mars, Jupiter, Saturn etc. (Berger, 1978). High orbital eccentricity (more elliptical) produces strong seasonal contrast due to highly modulated precession values, while low change in eccentricity has a significant role on solar radiation (insolation) received (larger) by the outer atmosphere at the perihelion and aphelion. At present, it is 3.5%, and difference in insolation increases when eccentricity is greater and vice versa. At the maximum eccentricity (0.06) the difference in the insolation received by the outer atmosphere between the day at perihelion and that of the day at aphelion can be as high as 30%. MTM spectral analysis of the last 3Ma eccentricity data reveals significant cycles at ~400-, 126-, and 95-ka, which are reconstructed and compared with original eccentricity time series (Fig. 8D-E). Two minor eccentricity cycles at ~69- and 54-ka are also evident, which were mentioned by Berger (1977, p. 45) as its combined effect with tilt and precession. Normalized cumulative effect of eccentricity, tilt and precession is defined as the ETP, which causes orbital forcing on climatic changes. MTM results of the ETP for last 3-Ma exhibit triplets of the ~400, 126-, 95-ka eccentricity, ~54-, 41-, and 31-ka tilt, ~23-, 19- and 17-ka precession, and 15- and 13-ka suborbital cycles (Fig. 8G).

Earth's wobble/precession:

While rotating on its axis on the orbital path, Earth wobbles like a spinning toy-top (gyrating motion) as a result from a torque generated by gravitational forces of the Sun and Moon together acting on the slight equatorial bulge of the Earth (Fowles, 1977). This gyrating motion of Earth's rotational axis is due to tidal forcing by Sun and Moon on the oblate-spheroid shape of Earth. Due to this torque, Earth moves slightly backwards (precess) with wobble, and it nearly takes ~25,700 years to come back at the same point. This wobbling backward motion of Earth is known as precession (p) (Fig. 8A-c, B). It is defined as $p = e \sin \omega$, where ω is Sun's longitude of perihelion with respect to moving vernal equinox. Earth's rotational axis at present points towards Polaris (North Star) during the precession maximum, but it pointed towards Vega during precession minimum at ~12.5-ka (Fig. 8B). At present northern hemisphere has winter when Earth is closest to Sun due to

combined effect of tilt and precession, but at ~12.5-ka it had winter when Earth was farthest from Sun. Furthermore, the Earth's orbital ellipse itself precesses in space of arc at ~51'/year due to gravitation perturbation of Jupiter, Saturn and other larger planets. This orbital precession shortens the period of precession of equinoxes with respect to perihelion from ~25-ka to 23-ka (Berger, 1978, 1993). Variation in precession of equinoxes during the last 3 Ma is presented (Fig. 8D), and its MTM spectrum reveals the 23-, 19-, and 17-ka cycles (Fig. 8G).

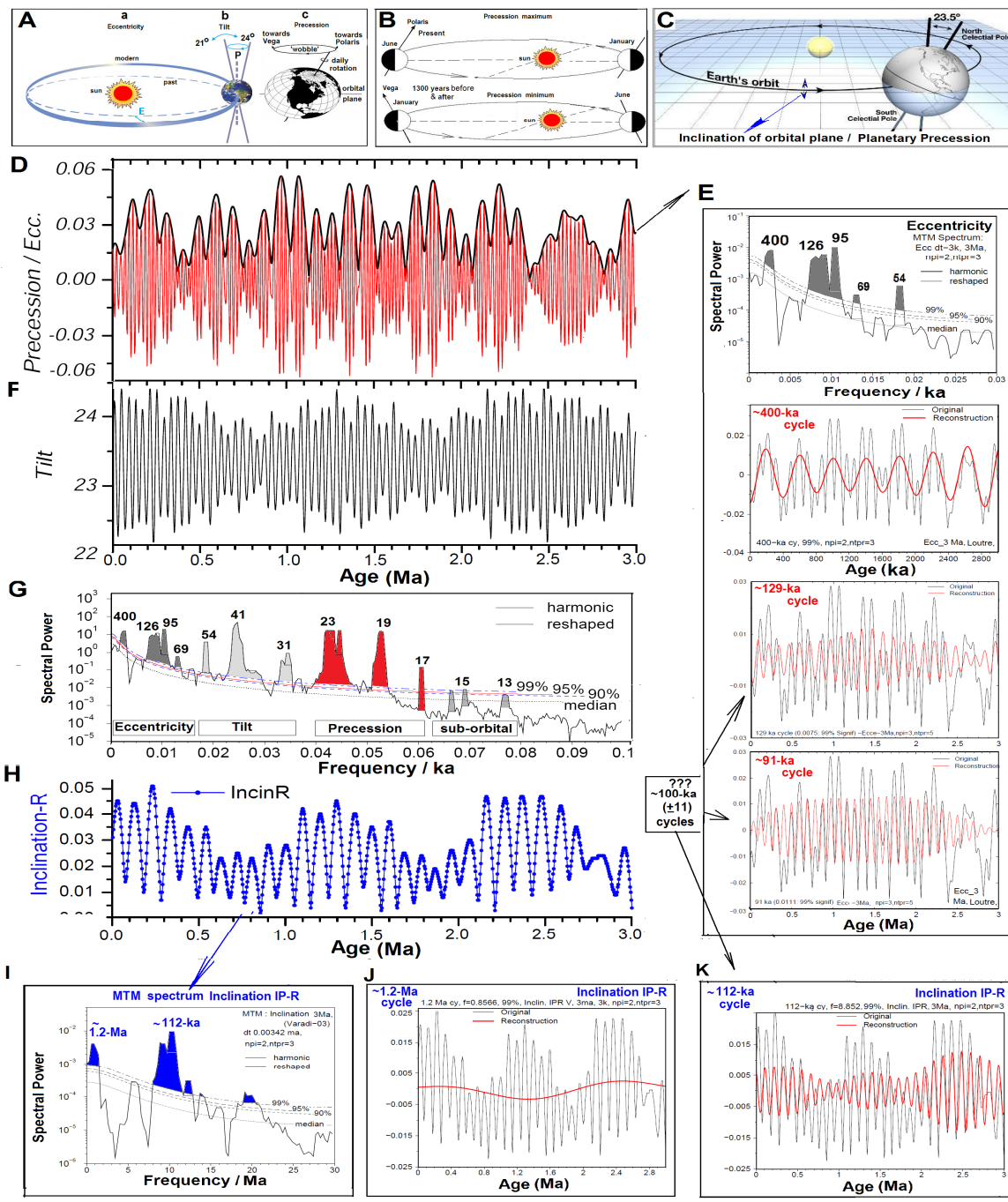


Fig. 8: Earth's orbital changes in the (A) eccentricity (a), tilt (b) and precession (c) (Berger, 1978). At present precession maximum axis points to Polaris, while it pointed to Vega at ~12.5-ka (B). Orbital inclination (C). Changes in eccentricity and precession during the last 3-Ma (D). MTM spectral power (upper) along with comparison in original and reconstructed cyclic components of ~400-, 129-, 91-ka eccentricity (lower) cycles (E). Tilt during last 3-Ma (F). MTM of combined effect of the Earth's orbital forcing "ETP" showing triplets of the ~400-, 129-, 91-ka eccentricity, 54-, 41- and 31-ka tilt, 23-, 19-, 17-ka precession, and the suborbital ~15- and 13-ka cycles (G). Orbital inclination relative to the invariable plane (Varadi *et al.*, 2003) in radians (H), and its MTM spectrum showing cycles at ~1200- and 112-ka cycles (I), and the reconstructed ~1.2-Ma (J) and 112-ka (K) cyclic components. Note the differences in amplitude changes in the ~129-ka and 91-ka cycles due to eccentricity (E), and ~112-ka cycles due to inclination (K), and all are the so called ~100-ka (± 11 -ka) cycles. Figures (A-C) are modified after their sources (www.wikipedia.com).

Earth's axial tilt:

Earth's rotational axis is tilted at $\sim 23.4^\circ$ at present with respect to the perpendicular on the orbital plane and it is known as axial tilt/obliquity (t, Fig. 8A-b, C). During December axis is tilted away from the Sun, while in June it is tilted towards the Sun, resulting in northern hemisphere tilted at lesser angle and receives more radiation causing northern summer and vice versa. If the axial tilt would have been zero, there would not have been any seasons on Earth. Reason for axial tilt is not certain, but few astronomers are of opinion that ~5 billion years ago (Ga), the infant Earth was struck by a Mars size planet badly, which not only tilted its axis, but also split apart a mass which formed its satellite, the Moon. It was blessing in disguise, as seasons on Earth are due to axial tilt. At times of lesser tilt (22°) high latitudes receive lesser Sun light than during higher tilt periods, and thereby altering the climate in term of expanded ice-sheets at the poles and causing the ice-ages. In the last 3-Ma, it varied between 22° - 24.5° (Fig. 8F), and its MTM results produce well known the ~54-, 41-, and 31-ka tilt cycles (Fig. 8 G).

Earth's orbital plane's inclination:

The 4th orbital element is inclination (i) of the Earth's orbital plane that moves up and down relative to its present position (Fig. 8C). It is termed as precession of the ecliptic or planetary precession. Up and down motion of Earth's orbital plane with respect to solar orbital plane also moves with respect to the orbits of the other planets, mainly Jupiter, because the invariable plane (angular momentum of the solar system) is almost same to the orbital plane of Jupiter. Researchers suggested that a disk of dust and other planetary debris exists in the invariable plane, and it affects the Earth's climate in several ways. Earth moves through this invariable plane at 9th January and 9th July each year at present, when there are reports with increased radar-detected meteorites and meteoritic dust clouds. Inclination of the Earth's orbital plane was not a part in the Milankovitch's theory of climate change. Inclination has a strong (68% variance) ~100-ka cycle, which is very similar to the ~100-ka eccentricity cycles recorded in global ice volume during late Quaternary ice ages (Hays *et al.*, 1976).

Quinn *et al.* (1991) calculated inclination of Earth's orbital plane, which was used by Muller and McDonald (1997a,b) to challenge the 100-ka glacial cycles not by the eccentricity but due to inclination. Varadi *et al.* (2003) refined inclination values, which are presented for the last 3-Ma (Fig. 8H). MTM spectrum of inclination suggest cycles at ~1.2-Ma and 112-

ka (Fig. 8I), and cyclic components are reconstructed and compared with original time series (Fig. 8 J-K). The eccentricity and inclination of orbital plane, both share the common forces, i.e., the gravitational perturbation and torque forces exerted by Jupiter and extra Jovian planets in the Earth's orbital dynamics through out the geological past. The climate change on Earth is influenced by the gravitational pull/push (perturbation) of the planets at daily (tidal), monthly (soli-lunar), seasonal (rain), annual (ENSO), decadal (Sunspots), and millennial (amplitude modulated Sunspot cycles in Figs. 6-7) to the orbital scales (Figs. 9-10). Orbital and sub-orbital cycles in monsoon in the radiolarian records are documented by Gupta (1999, 2002, 2003, 2009).

Solar Insolation:

Solar radiation (insolation) arriving at the top of surface of Earth at a given latitude and time is computed based on Earth's eccentricity (e), tilt (t), and Sun's longitude of perihelion (ω) with respect to moving vernal equinox (Berger, 1978). Influence of eccentricity and precession are mostly found everywhere, but dominant in the tropics, whereas tilt is more dominant in the polar/sub-polar regions (Berger, 1993). Insolation is straight and high during summer at the tropics when Earth is closer to perihelion (nearest point - 21st June) and low during winter when it is near aphelion (farthest point - 21st December) in its orbit around Sun at present (but not in the past), whereas polar regions receive radiation at an angle due to the axial tilt (Fig. 5A-d). When insolation is higher at 30°N over India during summer, southern Indian Ocean receives it lesser being austral winter at 30°S between Australia and Madagascar (Fig. 2C). It creates inter-hemispheric land-sea thermal contrast, generating low and high atmospheric pressure resulting into the stronger monsoon, and opposite happens with low summer insolation resulting into weak monsoon.

Researchers used insolation values of 21st June at 65°N for comparing their time series data, whereas as Berger (1977, 1993) strongly recommended monthly/seasonal and regional insolation, especially if time series are from tropic/subtropics. Leuchner and Sirocko (2003) and Gupta (2003, 2009) considered 30° insolation difference between two hemispheres ($\delta-I=30^\circ\text{N}$ minus 30°S) during northern summer as the insolation monsoon index (IMI), and they found very good relation with monsoon proxies. As differential solar heating of the mid latitudes during northern summer (Fig.1) results in the monsoonal rains, a time series of differential solar insolation ($\delta-I$, 30°N-30°S) during 21st April-21st July (90 days mean) as Indian summer monsoon index (ISM) is calculated at 1-ka for the last 10-Ma using insolation equations of Berger and Loutre (1991) in the Analyseries (Pailard et al., 1996), and presented in Fig. 9A.

MTM spectral analysis of $\delta-I$ revealed highly significant triplet cycles of eccentricity (~95-, 100-, 400-ka), tilt (~54-, 41-, 31-ka), precession (~23-, 19-, 17-ka), and sub-orbital cycles at ~15-, 13-, 11-, 10-, and 9-ka (Fig. 9B). MTM spectral analyses of (-I) revealed highly significant triplet cycles of eccentricity (~95-, 100-, 400-ka), tilt (~54-, 41-, 31-ka), precession (~23-, 19-, 17-ka), and sub-orbital cycles at ~15-, 13-, 11-, 10-, and 9-ka (Fig. 9B). Significant cyclic components of the ~400-, 126-, and 95-ka eccentricity, 54-, 41-, 31-ka tilt, and 23-ka precession in the (-I) are reconstructed and exhibited (Fig. 9C-I). Bell (2003) analyzed 800-ka climatic record comparing with precession signals and concluded that the 30-ka cycle could also be due to precession-related summer solar heat response affecting the global climates. It is in contrast to the established notion that the ~31-ka cycle (Fig. 9H) is due to tilt (Berger, 1977; Gupta, 2009), which is also evident in spectral analysis of tilt (Fig. 8-G).

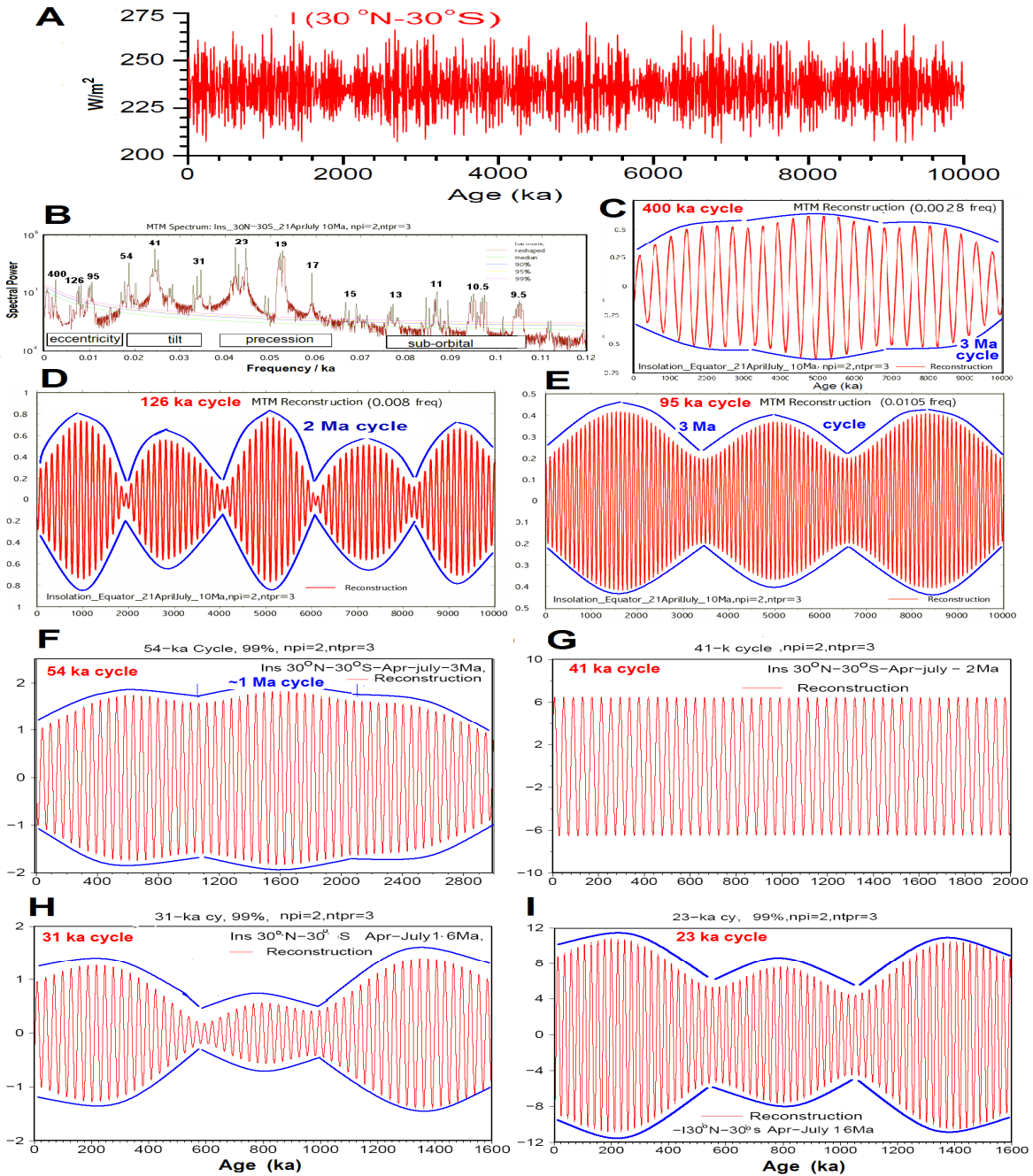


Fig. 9: (A) The δ -I monsoon index for the last 10-Ma, and (B) its MTM spectrum showing significant triplet cycles of the eccentricity (\sim 95-, 126-, 400-ka), tilt (\sim 54-, 41-, 31-ka), precession (\sim 23-, 19-, 17-ka), and sub-orbital cycles at \sim 15-, 13-, 11-, 10-, and 9-ka. MTM reconstruction of equatorial summer isolation for last 10-Ma exhibiting the cyclic components of the \sim 400-ka (C), 95-ka (E) with amplitude modulated \sim 3-Ma cycle, whereas 126-ka (D) has amplitude modulated \sim 2-Ma eccentricity cycles. MTM reconstruction of δ -I exhibits cyclic components of 54-ka with amplitude modulated cycle of \sim 1-Ma in the last 3 Ma (F), and (G) 41-ka cycle with uniform amplitude in last 2 the Ma. Reconstructed δ -I exhibiting 31-ka tilt (H) and 23-ka precession (I) components with amplitude modulated 600-ka cycle in last 1.6 Ma.

Triplet cycles of Earth's eccentricity in the Monsoon:

Earlier, typical ~23-, 41, and 100-ka Milankovitch (1941) cycles were reported in the Indian monsoon by Clemens et al. (1991), Kroon et al. (1991), Prell et al. (1992), Prell and Kutzbach (1992) and their groups. Triplet cycles of eccentricity at ~400, 126, and 95-ka (Fig. 8E) were forecasted by Berger (1977, cf. table 3), and they are evident in MTM results of the δ -I monsoon index (Fig. 9B). These triplet eccentricity cycles were first reported in radiolarian transfer function based monsoonal SSTs (August) from the central tropical Indian Ocean (Gupta et al., 1996). Subsequently, these were reported from the $\delta^{18}\text{O}$ (Clemens and Tiedemann, 1997), foraminiferal abundance (Muller and McDonald, 1997a-b) in western tropical warm pool, and in the monsoonal radiolarian indices (Gupta, 1999, 2002, 2003, 2009). Later, Gupta et al. (2001) have reported ~412-, 121- and 94-ka triplets cycles from benthic foraminifer *U. proboscidea* monsoon proxy from DSDP-214 site in the eastern Indian Ocean.

Milankovitch cycles in the Monsoon:

Clemens et al. (1991) and Prell et al. (1992) and their group established the role of ~23-ka precession, ~41-ka tilt and ~100-ka eccentricity cycles in the proxy monsoonal records of *G. bulloides*, CaCO_3 , organic carbon and barium contents from the Arabian Sea upwelling zone. These three cycles are primarily known as the Milankovitch (1941) cycles in the Indian monsoon. Beaufort et al. (1997) studied abundance variation in the coccolithophores (*Florisphaera profunda*), an index of oceanic primary productivity, and reported the ~100-ka eccentricity and ~23-ka precession cycles, and they related it to insolation response in monsoonal productivity in the equatorial Indian Ocean. Gupta (1996) reported that modern radiolarian faunal assemblages characterized the overlying surface water SST and salinity, and clearly divide high salinity equatorial and low salinity distal Bay of Bengal waters in the central Indian Ocean. Gupta et al. (2002) studied radiolarian fluxes from the sediment traps moored in the southern Bay of Bengal suggested that radiolarians were invariably higher at times of higher sea surface temperature ($\text{SST} \geq 28^\circ\text{C}$) and moderately lower salinity (~33.5 psu) during the summer prior to monsoon of 1991-93. These studies suggested that higher SSTs due to summer heat and lower salinity due to rains might affect radiolarian fluxes during the monsoon. Down core studies revealed that the salinity sensitive radiolarians (Rads/g, Pyloids, *Spongaster*, *Stylodictya-Stylochlamydidium*, and *Anthocyrtidium* assemblages) changed cyclically at ~126-, 95-ka due to Earth's orbital eccentricity, ~54-, 41-, and 31-ka due to axial tilt, ~23-, 19-, and 17-ka due to changes in the precession of equinoxes, besides the ~15-, 13- and 11-ka sub-Milankovitch cycles in the last 485-ka (Gupta and Fernandes, 1997; Gupta, 1999, 2002, 2003, 2009). Besides, the reconstructed cyclic components of Rads/g also revealed a conspicuous change in the trends of the amplitudes of ~95-, 54-, 41-, 17-, 15-, and 13-ka cycles suggesting an effect of the mid-Brunhes climate shift at ~300-350-ka (Gupta, 2009). Similar mid-Brunhes climate shift is later found in the variation of *G. bulloides* from DSDP Hole 716A and 728B by Gupta et al. (2010).

Supra Milankovitch (>100-ka) cycles in the Monsoon:

The cycles >100-ka are termed as supra-Milankovitch cycles, and are mainly the response to the triplet eccentricity cycles, which were first reported in radiolarian transfer function based monsoonal SSTs (August) from the central tropical Indian Ocean (Gupta et al., 1996). Later, Gupta et al. (2001) reported ~100-ka and 400-ka Earth's eccentricity

from benthic foraminiferal monsoon proxies (DSDP-214 site), and Gupta and Melice (2003) found them in benthic foraminifers *U. proboscidea* and *E. exigua* from ODP-758 in the eastern equatorial Indian Ocean. Banerjee *et al.* (2010) documented the ~ 400 -ka eccentricity cycles in the Na, Mg, Cu, Co, and Ni (Fig. 10 A-C, Ni) micronutrients carried away to sea-floor by scavenging during the monsoonal productivity, in a slowly accreting hydrogenous ferro-manganese crust dating back to ~ 3.5 Ma from Vityaz fracture zone in equatorial Indian Ocean. Ni is considered un-common in terrestrial sources and it is always higher in extra-terrestrial cosmic/meteorite dust ($<1 \mu\text{m}$) flux into the ocean. They related these changes due to the monsoonal oceanic productivity, which is known to vary with insolation variance at ~ 100 -ka eccentricity cycles in the equatorial Indian Ocean (Beaufort *et al.*, 1997). Monsoonal productivity induced fecal pellets and the particulates incorporated the micronutrients of Ni, presumably derived from cosmic (comet/meteoritic) dust, and transported it to the ocean floor on the Fe-Mn crust.

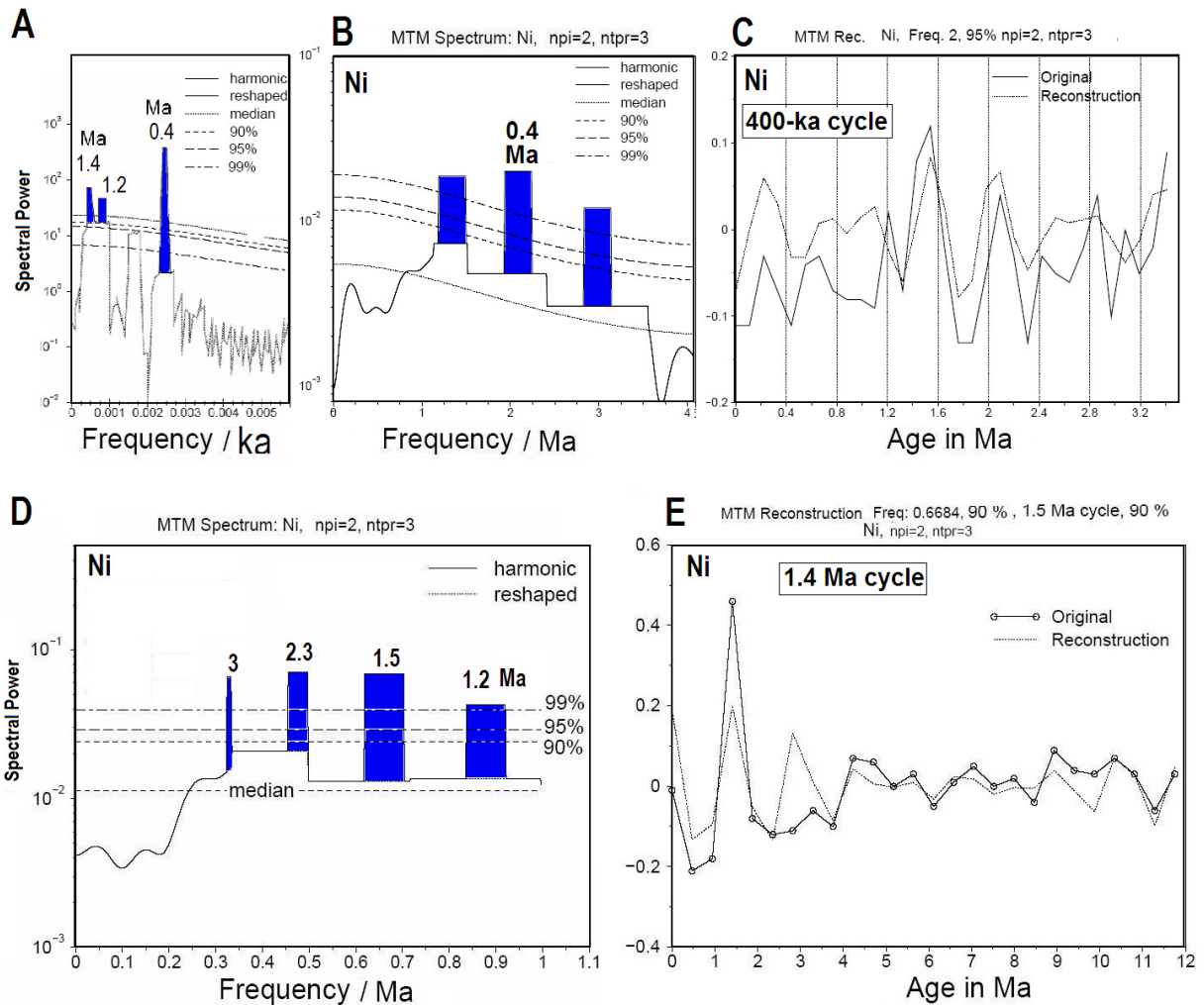


Fig. 10: (A) A part of MTM spectral analysis of δ -I monsoon index sampled at ~ 100 -ka interval showing significant cycles of ~ 1.4 and 0.4 Ma eccentricity cycles. (B) MTM of Nickel in Vityaz fracture zone (Banerjee *et al.*, 2010) showing ~ 400 -ka cycle, which is reconstructed and compared with original Ni time series (C). (D) MTM of Nickel from Central Indian Ocean Basin exhibiting significant ~ 3 , 1.5 , and 1.2 Ma

cycles (Banerjee *et al.*, 2008) as predicted by Berger (1977, cf. table 3), and only 1.5 Ma cycle is reconstructed and compared with original Ni time series (E).

Banerjee *et al.* (2008) presented elemental variation in layers of a slow accreting hydrogenous crust having a record of the last ~12 Ma from the central Indian Ocean. Red-fit and MTM spectral analyses of Fe, Mg and Ni revealed the existence of significant (>90%) cycles at ~3, 1.5, and 1.2 Ma (Fig. 10 D-E, Ni). As the Fe/Ni ratio was higher than oceanic nature, they attributed to high Ni contents from the cosmic dust flux, which incidentally is known to have similar cycles (Johnson, 2001), supported by propositions that an estimated 5-700 small diameter meteorites are entering into Earth every Ma (Nurmi *et al.*, 2001). They suggested that the Fe, Mg, and Ni cycles at ~3, 1.5 and 1.2 Ma (main peak 1.3 Ma) could be result of geochemical response to similar 3.5-, 1.3-Ma eccentricity cycle (Berger, 1977, cf. table 3) related solar insolation changes, which are shown as the amplitude modulated envelop of bundles in the ~400-, 126-, 95-ka (eccentricity) and 54-ka (tilt) cycles (Fig. 9C-F), and at ~3, 1.5 and 1.2 Ma supra-Milankovitch cycles in the Ni contents (Fig. 10).

Oldest Indian Monsoon record

Origin of the monsoon in geological past has been enigmatic. Probably, one of the earliest paleo-monsoon scenarios presented was from the radiolarian faunal assemblage changes during the late Miocene (~6-8.8 Ma) from the Sawai Bay Formation, Neill Island, Andaman (Gupta and Nigam, 1988; Guptha *et al.*, 1988) in the 1st International Conference on Radiolaria held at Marburg, Germany. A year later, Quade *et al.* (1989) reported development of Asian monsoon as revealed by the marked ecological shift from grassland to shrub vegetation (C-4) proxy variation in the molar contents of mammals during the late Miocene ~8-Ma from deposits in the northern Pakistan. Thereafter, series of papers appeared describing changes in abundance of the upwelling foraminifers like *G. bulloides*, and radiolarians like *Collosphaera Sp. A.* in the sediments from Off Oman Margin (Kroon *et al.* 1991; Prell *et al.*, 1992). Gupta (S.M.) and Srinivasan (1992) reported upwelling radiolarian fauna and the diatom blooms at ~6-8.5 Ma, and discussed the basinal shallowing due to enhanced supply of sediments derived by the Ganges and Brahmaputra rivers into Andaman Sea. Gupta (A.K) and Srinivasan (1992a-b) found foraminiferal changes at ~9-Ma, which they related to monsoonal productivity in the Andaman Islands. As those foraminiferal, radiolarian and diatom species are abundance in modern monsoon dominated upwelling areas, these authors suggested that the monsoon strengthened at ~8.5 Ma in the region. Later, Gupta and Fernandes (1995) derived the long range radiolarian transfer function for the SST during August and surface salinity during July-August monsoonal peak season, and they estimated the paleo-salinity using Neill Island radiolarian data during the Late Miocene. They found that the monsoonal salinity was higher at ~8.5-Ma and lower at ~6-Ma in the Bay of Bengal, and attributed it to the lowering of the surface salinity due to enhanced river runoff by the Indian rivers (Ganges and Brahmaputra) into the Bay of Bengal. Similarly, Chen *et al.* (2003) found that changes in radiolarian flux, especially in abundance of Pyloniids, are good proxies and analogues to modern upwelling summer monsoon radiolarians. They suggested that the east Asian summer monsoon first initiated close to the middle/late Miocene boundary at ~12-11-Ma and then strengthened at ~8.24-Ma, which is in conformation with earlier studies from the Andaman Islands (Gupta (SM) and Srinivasan (1992). Since then, numerous papers have been published establishing the existence of the late Miocene monsoon in the Arabian Sea and Indian Ocean. However, Guo *et al.* (2002) proposed that the eolian loess of central China is much older (22 Ma) than believed so far at ~8-Ma, implying that monsoon could still be older. Clift *et al.* (2004)

studied variations in clay minerals in South China Sea and suggested alterations from drier to wetter climate before ~15-Ma. The timing of initial monsoon strength/origin is still not un-disputed in the global climate system.

Conclusion

Although Indian monsoon mostly sets on in early June, it often deceives casting droughts or floods causing hardship to millions in the Indian subcontinent. It varies at the intra-monsoonal scale with 40-50 days cycle due to variability in the ITCZ/Hadley cell cloud formation and its migration towards Indian subcontinent. It exhibits cycles at ~2.7, 3.5 (QBO), 5, 7, (El-Nino/La-Nina, ENSO), 9, 11, 22, 30, 45, 60, 80, 95, 150, 180, 245, 584, 1100, and 2200 years cycles, mainly reported due to Sunspot activity. Monsoon records also suggest variability due to Sun-Moon tidal effect at 8.9, 13.6, 18, 27.2, 44, 90-95, 180, 1470, 1800, and 5000 years cycles. Besides, monsoon also varies at the sub-Milankovitch/sub-orbital (~7-, 9-ka, 11-, 13- and 15-ka), Milankovitch/orbital (100-ka eccentricity, 54-, 41-, and 31-ka tilt, and 23-, 19- and 17-ka precession of equinoxes), and the supra Milankovitch (1.3 Ma and 0.4-Ma) eccentricity cycles. There are growing body of evidences implying that the changes in trade wind strength, which later transform into monsoonal winds (Fig. 2A), are also influenced by the solar heating/irradiance/insolation of the tropical/subtropical sea surface temperatures, resulting into evaporation and cloud formation. So also, there are several proxy monsoon records suggesting an important role of solar insolation (also Sunspots) in influencing the monsoon sensitivity forcing to vary it on seasonal, yearly, decadal, centennial, millennial and astronomical time scales. Several evidences exhibiting reasonable relations/rationales for monsoonal influences, like (i) Sunspots, (ii) synod effect, (iii) seasonal insolation and micro variations in the Earth's eccentricity and precession (Bertrand *et al.*, 2002), and (v) tidal forcing etc., are known to affect the monsoon strength, but to date these are not considered as the input parameters in predictive models of monsoon, either due to inconsistency in their correlation coefficients with time or difficulties in handling new variables in complex models. There seems to be a wealth of literature and historical account scattered in ancient scriptures on monsoon rains, its cyclic nature enabling pre-emptive mitigation measures adopted by rulers for benefit of the agrarian subject. For example, Kautilya used to reduce taxes on agriculture during poor monsoon, declare community feast (Sadaa-vart) during famine etc. as narrated in Artha-Sastra (Waldauer *et al.*, 1996). Due to numerous physical forcings interacting on monsoon at the same time, and their linear and non-linear response are not fully understood and assimilated in monsoon predictive models with high reliability at least at weekly level, so the farmers can plan their crops in better way. With such an advance in knowledge, when monsoon fails (flood/drought), it makes us to realize that we do not know for sure - how would be next monsoon with reasonably dependent limit of uncertainties.

Acknowledgements: Author thank to the Director, NIO, Goa, and the Director General, Council of Scientific & Industrial Research (CSIR), New Delhi for support. He thankfully acknowledges several sources for the illustrations modified after original graphics from www.wikipedia.com, www.google.com, www.ngdc.noaa.gov/paleo/forcing.html, Sunspot numbers (www.sidc.be), and paleo-TSI and Sunspot numbers (www.noaa.edu/paleoclimatology) and used in MTM analyses and creating the graphics used in the paper. Author thanks to Marie Loutre (Institute of Astrophysics & Astrodynamics, Brussels) for digital data on eccentricity, precession and tilt for the last 3 Ma, and Rajesh Agnihotri for sparing All India Homogenized Rain Fall Data (www.tropmet.res.in/static_page.php?page_id=53). Article is dedicated by the author to Prof. Björn A. Malmgren (Nörttlje, Sweden) on the GURU-POORNIMA occasion as a gratitude for his teachings on quantitative paleoceanography, artificial neural networks, multivariate and the time series spectral analyses, and invoking the naturalistic views in the author. It is a part of N.I.O's on going Project GAP 2175/OLP 0011 on understanding the geology of the deep-sea oceans (N.I.O.'s contribution no./ref No. 4840).

References

- Agnihotri, R. and Dutta, K. (2003) Centennial scale variations in monsoonal rainfall (Indian, east equatorial and Chinese monsoons): Manifestations of solar variability. *Curr. Sci.*, v. 85, pp. 459–463.
- Agnihotri, R., Altabet, M. A., Herbert, T. D. and Tierney, J. E. (2008) Subdecadally resolved paleoceanography of the Peru margin during the last two millennia. *Geochem. Geophys. Geosyst.*, v. 9, pp. Q05013, doi:10.1029/2007GC001744.
- Agnihotri, R., Dutta, K., Bhushan, R. and Somayajulu, B.L.K. (2002) Evidence of solar forcing of the Southwest monsoon during the last Millennium. *Earth Planet. Sci. Lett.*, v. 198, pp. 521-527.
- Ashok, K., Guan, Z. and Yamagata, T. (2001) Impact of the Indian Ocean dipole on the relationship between the Indian monsoon rain fall. *Geophys. Res. Lett.*, v. 28, pp. 4499-4502.
- Banerjee, R. Gupta, S. M., and Miura, H. (2008) A million year cycle in the Fe, Mg and Ni records of a ferromanganese crust from the equatorial Indian Ocean. AGU fall meeting, San Francisco, pp. PP43A-1511.
- Banerjee, R., Gupta, S. M., Miura, H. and Borole, D. V. (2010) A ~400 ka supra-Milankovitch cycle in the Na, Mg, Pb, Ni, and Co records of a ferromanganese crust from the Vityaz fracture zone, central Indian ridge. *Climate of the Past – Disc.*, v. 6, pp. 1311-1335, <http://direct.sref.org/1814-9359/cpd/2010-6-1311>
- Bard, E., Raisbeck, G., Yiou, F. and Jouzel, J. (2000) Solar irradiance during the last 1200 years based on cosmogenic nuclides. *Tellus, Ser. B*, v. 52, pp. 985–992, doi:10.1034/j.1600-0889.2000.d01-7.x.
- Beaufort, L., Lancelot, Y., Chamberlain, P., Cayre, O., Vincent, E., Bassinot, F. and Labeyrie, L. (1997) Insolation cycles as a major control of equatorial Indian Ocean primary production. *Science*, v. 278, pp. 1451–1454.
- Ber, J., Baumgartner, S., Hannen-Dittrich, B., Hauenstein, J., Kubik, P. P., Lukasczyk, C., Mende, W., Stellmacher, R. and Suter, M. (1994) The Sun as a variable star: Solar and stellar irradiance variations. In: *Pap, J.M., et al., (eds.)*, Cambridge University Press, Cambridge, pp. 291.
- Bell, G.J. (1977) Changes in sign of the relationship between Sunspots and pressure, rainfall and the monsoons. *Weather*, v. 32, p. 26-32.
- Bell, L. G. (2003) A 30,000 yr precession-related cycle affecting climate. *Theor. Appl. Climatol.* v. 74, pp. 245–253, DOI 10.1007/s00704-002-0711-7.
- Berger, A. L. (1977) Support for the astronomical theory of climatic change. *Nature*, v. 269, pp. 44-45.
- Berger, A.L. (1978) Long term variations of daily insolation and Quaternary climatic changes. *J. Atmos. Sci.*, v. 35, pp. 2362-2367.
- Berger, A.L. (1993) Insolation and Earth's orbital periods. *J. Geophys. Res.*, v. 98, D6, pp. 10341-10362.
- Berger, A.L. and Loutre, M.F. (1991) Insolation values for the climate of the last 10 million years. *Quaternary Sciences Review*, v.10, pp. 297-317.
- Bertrand, C., Loutre, M. F. and Berger, A. (2002) High frequency variations of the Earth's orbital parameters and climate change. *Geophys. Res. Lett.*, v. 29, pp. 1893-1996, doi:10.1029/2002GL015622.
- Bond, G. B., Kromer, B., Beer, J., Muscheler, R., Evans, M. N., Showers, W., Hoffmann, S., Lotti-Bond, R., Hajdas, I. and Bonani, G. (2001) Persistent solar influence on North Atlantic climate during the Holocene. *Science*, v. 294, pp. 2130–2136, doi:10.1126/science.1065680.
- Burgess, E. (1860) *The Surya Siddhanta – English Translation 1989*, Gangooly, P., ed., Motilal Banarsidass, Delhi.
- Burroughs, W.J. (2003) *Weather cycles real or imaginary*. Cambridge University Press, UK, p. 325.
- Chakraborty, P.K. and Bondyopadhyay, R. (1986) Solar effect on rainfall in West Bengal. *Mausam*, v. 37, pp. 251-258.
- Chao W. C. and Chen, B. D. (2001) The origin of monsoon. *J. Atmos. Sci.*, v. 58, pp. 3497-3507.

- Chen, M., Wang, R., Li, H-Y., Han, J. and Lu, J. (2003) Development of east Asian summer monsoon environments in the late Miocene: radiolarian evidence from Site 1143 of ODP Leg 184. *Marine Geol.*, v. 201, pp. 169-177.
- Chen, T-C, Tzeng, R-Y. and Yen, M-C. (1988) Development and life cycle of the Indian monsoon: Effect of the 30–50 day oscillation. *Mont. Weather Rev.*, v. 116, pp.2183-2199.
- Choudhury, A, Abhayankar, V.P. and Phadke, M.V. (1981) Solar activity as a potential factor for fore-shadowing drought in Indian summer monsoon regime. *Mausam*, v. 32, pp. 277-280.
- Clark, C.O., Cole, J.E. and Webster, P.J. (2000) Indian Ocean SST and Indian summer rainfall: predictive relationships and their decadal variability. *J. Climate*, v. 13, pp. 2503-2519.
- Clemens, S.C. (1998) Dust response to seasonal atmospheric forcing: proxy evaluation and calibration. *Paleoceanography*, v. 13, pp. 471-490.
- Clemens, S.C. and Tiedemann, R. (1997) Eccentricity forcing of Pliocene-Pleistocene climate revealed in a marine oxygen isotope record. *Nature*, v. 385, pp. 301-304.
- Clemens, S. C., Prell, W. L., Murray, D., Shimmield, G. and Weedon, G. (1991) Forcing mechanisms of the Indian Ocean monsoon. *Nature*, v. 353, pp. 720–725.
- Clift, P.D., Layne, G.D. and Blusztajn, J. (2004) Marine sedimentary evidence for monsoon strengthening, Tibet uplift and drainage evolution in East Asia, In: *Continent-Ocean Interactions within East Asian Marginal Seas*. *Geophys. Monogr.*, Ser. v. 149, 10.1029/149G14, pp. 255-282.
- Currie, R.G. and Fairbank, R.W. (1985) Periodic 18.6 year and cyclic 11 year induced drought and flood in north eastern China and some global implications. *Quat. Sci. Rev.*, v. 23, pp. 109-134.
- deMenocal, P.B. (2004) African climate change and faunal evolution during the Pliocene-Pleistocene. *Earth Planet. Sci. Lett.* v. 220 pp. 3-24.
- Eddy, J.A. (1977) Climate and the changing Sun. *Climatic Change*, v. 1, pp. 173-190.
- Eddy, J.A. and Boornazian, A. A. (1979) Secular decrease in the solar diameter 1863-1953. *Bull. Amer. Astron. Soc.*, v. 11, pp. 437.
- Eddy, J.A., Gilliland, R.L. and Hoyt, D.V. (1982) Changes in the solar constant and climatic effects. *Nature*, v. 300, pp. 689-693.
- Feynman, J. and Fougere, P.F. (1984) Eighty eight year periodicity in solar-terrestrial phenomena confirmed. *J. Geophys. Res.*, v. 89, pp. 3023-3027.
- Fowles G.R. (1977) *Analytical mechanics*. 3 edition. New York, Holt, Rinehart and Winston, ch. 8, p. 243.
- Gadgil, S. (1988) Recent advances in monsoon research with particular reference to the Indian monsoon. *Aust. Meteorol. Mag.*, v. 36, pp. 193–204.
- Gadgil, S. (1996) Climate change and agriculture-An Indian perspective, In *Climate Variability and Agriculture*. (eds.), *Y. R. Abool, S. Gadgil and G. B. Pant*, pp. 1-18, Narosa, New Delhi, India.
- Gadgil, S. (2003) The Indian monsoon and its variability. *Ann. Rev. Earth Planet Sci.*, v. 31, pp. 429-467.
- Gadgil, S., Joseph, P.V. and Joshi, P.V. (1984) Ocean-atmosphere coupling over monsoon regions. *Nature*, v. 312, pp. 141-143.
- Gadgil, S. Srinivasan, J., Nanjundiah, R.S., Kumar, K.K., Munot, A.A. and Kumar, K.R. (2002) On forecasting the Indian summer monsoon: the intriguing season of 2002. *Curr. Sci.*, v. 43, pp.394-403.
- Ghil, M., Allen, M.R., Dettinger, M.D., Ide, K., Kondrashov, D., Mann, M.E., Robertson, A.W., Saunders, A., Tian, Y., Varadi, F. and Yiou, P.(2001) Advanced spectral methods for climatic time series. *Rev. Geophys.*, v. 40, pp. 1-23.
- Gilliland, R.L. (1981) Solar radius variations over the past 265 years. *Astrophys. J.*, v. 248, pp. 1144-1155.
- Gleissberg, W. (1958) The eighty years solar cycle in auroral frequency numbers. *J. British Astron. Asso.*, v. 75, pp. 227-231.
- Guo, Z. T., Ruddiman, W.F., Hao, Q. Z., Wu, H. B., Qiao, Y. S., Zhu, R. X., Peng, S. Z., Wei, J. J., Yuan, B. Y. and Liu, T. S. (2002) Onset of Asian desertification by 22 Myr ago inferred from loess deposits in China, *Nature*, v. 416, pp. 159-163.
- Gupta, A.K. and Mélice, J-L. (2003) Orbital forcing of the Plio-Pleistocene Indian monsoons: benthic foraminiferal proxies from ODP Site 758. *Curr. Sci.*, v. 85, pp.179-184.
- Gupta, A.K. and Srinivasan, M.S. (1992a) Deep-sea benthic foraminiferal changes and terminal Miocene event at tropical Indian Ocean DSDP site 214, *J. Geol. Soc. India*, v. 40, pp. 262-278.
- Gupta, A.K. and Srinivasan, M.S. (1992b) *Uvigerina*-*Proboscidae* abundances and Paleoceanography of the northern Indian Ocean DSDP site 214 during the late Neogene. *Marine Micropaleontol.*, v. 19, pp. 355-367.

- Gupta, A.K., Das, M. and Anderson, D.M. (2005) Solar influence on the Indian summer monsoon during the Holocene. *Geophys. Res. Lett.*, v. 32, pp. L17703, doi:10.1029/2005GL022685.
- Gupta, A. K., Dhingra, H., Mélice, J.-L. and Anderson, D.M. (2001) Earth's eccentricity cycles and Indian Summer monsoon variability over the past 2 million years: Evidence from deep sea benthic foraminifer. *Geophys. Res. Lett.*, v. 28, pp. 413-4134.
- Gupta, A.K., Sarkar, S., De, S., Clemens, S.C. and Velu, A. (2010) Mid-Brunhes strengthening of the Indian Ocean Dipole caused increased equatorial East African and decreased Australasian rainfall. *Geophys. Res. Lett.*, v. 37, pp. L06706, doi:10.1029/2009GL042225, 2010.
- Gupta, S.M. (1996) Quantitative radiolarian distribution in the surface sediment from the central Indian Ocean and their paleomonsoonal significances. *J. Geol. Soc. India*, v. 47, pp. 339-354.
- Gupta, S.M. (1999) Radiolarian monsoonal index Pyloniids respond to astronomical forcing in the last 5,00,000 years in the central Indian Ocean Basin. *Man & Environment*, v. 24, pp. 99-105.
- Gupta, S.M. (2002) Pyloniid stratigraphy – a new tool to date tropical radiolarian ooze from the central tropical Indian Ocean. *Marine Geology*, v. 184, pp. 85-93.
- Gupta, S. M. (2003) Orbital frequencies in radiolarian assemblages of the central Indian Ocean: implications on the Indian summer monsoon. *Palaeogeogr. Palaeoclimatol. Palaeoecol.* v. 197, pp. 97-112.
- Gupta, S.M. (2009) Radiolarian abundance - a monsoon proxy responding to the Earth's orbital forcing: Inferences on the mid-Brunhes climate shift, *Earth Science India*. v. 2, pp. 1-8. www.Earthscienceindia.info/Gupta.htm.
- Gupta, S.M. and Fernandes, A.A. (1995) Supra-generic radiolarian transfer function based late Miocene paleomonsoonal changes in the northeastern Tropical Indian Ocean. *Bull. Ind. Geol. Asso.*, v. 28, pp. 29-51.
- Gupta, S.M. and Fernandes, A.A. (1997) Quaternary radiolarian faunal changes in the central Indian Ocean: inferences to oscillating hydrographic front at 10°S of Equator. *Curr. Sci.*, v. 72, pp. 965-972.
- Gupta, S.M. and Nigam, R. (1988) Cluster analysis of radiolarian fauna from Sawai Bay Formation (Late Miocene), Neill Island, Ritchie's Archipelago, Andaman Sea, and its paleoceanographic significance. *Geologica et Palaeontologica*, conf. book - 1st Int. Conf. Radiolaria, (EURORAD V) Marburg, Germany, 21-24 July, 1988, p. 17.
- Gupta, S.M. and Srinivasan, M.S. (1992) Late Miocene radiolarian biostratigraphy and paleoceanography of Sawai Bay Formation, Neill Island, Andaman, India. *Micropaleontology*, v. 38, p. 209-236.
- Gupta, S.M., Fernandes, A.A. and Mohan, R. (1996) Tropical sea surface temperatures and the Earth's eccentricity cycles. *Geophys. Res. Lett.*, v. 23, pp. 3159-3162.
- Gupta, S.M., Mohan R. and Guptha, M.V.S. (2002) Radiolarian fluxes in the southern Bay of Bengal: A sediment trap study. *Deep Sea Res.*, I, v. 49, pp. 1669-1688.
- Guptha, M.V.S, Gupta, S.M. and Srinivasan, M.S. (1988) Calcareous Nannoplankton and radiolarian biostratigraphy of Sawai Bay Formation, Neill Island, Ritchie's Archipelago, Andaman Sea. *Geologica et Palaeontologica*, conf. book - 1st Int. Conf. Radiolaria, (EURORAD V) Marburg, Germany, 21-24 July, 1988, p. 18.
- Hadley, G. (1735) On the cause of the general trade winds. *Phil. Trans., R. Soc. London*, v. 34, pp. 58-62.
- Hale, G.E. (1924) The of Sunspot polarity. *Proc. National Acad. Sci., USA*, v. 10, pp. 53-55.
- Halley, E. (1686) A historical account of the trade winds and monsoons observable in seas between and near tropics with an attempt to assign a physical cause of the said winds. *Phil. Trans. R. Soc. London*, v. 16, pp.153-68
- Hameed, S., Yeh, W.M., Li, M.T., Cess, R.D. and Wang, W.C. (1983) An analysis of periodicities in the 1470-1974 Beijing precipitation record. *Geophys. Res. Lett.*, v. 10, pp. 436-439.
- Hari, K.C. (1997) True rationale of Surya Sidhanta. *Indian J. Historical Sci.*, v. 32, pp. 183-190.
- Hastenrath, S. (1987) On prediction of India summer rainfall anomalies. *J. Climate Appl. Meteor.*, v. 26, pp. 847-857.
- Hays, J.D., Imbrie, J. and Shackleton, N. (1976) Variations in the Earth's orbit: pacemaker of the Ice-Ages. *Science*, v. 194, pp. 1121-1132.
- Hiremath, K. M. (2006) The influence of solar activity on the rainfall over India: Cycle-to-cycle variations. *J. Astrophys. Astronom.*, v. 27, pp. 367-372.

- Hong, Y.T., Wang, Z.G., Jiang, H.B., Lin, Q.H., Hong, B., Zhu, Y.X., Wang, Y., Xu, L.S., Leng, X.T. and Li, H.D. (2001) A 6000-year record of changes in drought and precipitation in northeastern China based on a $\delta^{13}\text{C}$ time series from peat cellulose. *Earth Planet. Sci. Lett.*, v. 185, pp. 111.
- Hoyt, D. (1979) Variation in Sunspot structure and climate. *Climatic Change*, v. 2, pp. 79-92.
- Iyengar, R. N. (2009) Monsoon rainfall cycles as depicted in ancient Sanskrit texts. *Curr. Sci.*, v. 97, pp. 444-447.
- Johnson, K.S. (2001) Iron supply and demand in the upper ocean: Is extraterrestrial dust a significant source of bio available iron. *Global Biogeochem. Cycles*, v. 15, pp. 61- 63.
- Joseph, C.P. and Amatyia, B.V.S. (1986) Influence of long term changes in Sunspot activity on annual mean temperature over south India. *Mausam*, v. 37, pp. 276-278.
- Keeling, C.D. and Whorf, T.P. (2000) The 1,800-year oceanic tidal cycle: A possible cause of rapid climate change. *Proc. Nat. Acad. Sci., USA*, v. 97, pp. 3814-3819.
- King, J.W. (1973) Solar radius changes and the weather. *Nature*, v. 245, pp. 443-446.
- Kodera, K. (2004) Solar influence on the Indian Ocean monsoon through dynamical processes, *Geophys. Res. Lett.*, v. 31, pp. L24209, doi:10.1029/2004GL020928,
- Kroon, D., Steins, T. and Truett, S.R. (1991) Onset of monsoonal related upwelling in the western Arabian Sea as revealed by planktonic foraminifers. In *Prell, W.L. et al.*, Proceedings of the Ocean Drilling Project, College Station, Texas (Ocean Drilling Program), *Sci. Res.*, v. 117, pp. 257-263.
- Landscheidt, T. (1984) Cycles of solar flares and weather. In: N.-A. Morner and W. Karlen eds, *Climatic Changes on a Yearly to Millennial Basis*, D. Reidel Publishing Company, pp. 473-481.
- Leuschner, D.C. and Sirocko, F. (2003) Orbital insolation forcing of the Indian monsoon – a motor for global climate changes? *Palaeogeogr. Palaeoclimatol. Palaeoecol.*, v. 197, pp. 83-95.
- Meehl, G. A. (1987) South Asian monsoon and the tropospheric biennial oscillation. *J. Climate*, v. 10, pp. 1921-1943.
- Milankovitch, M.M. (1941) *Kanon der Erdbestrahlung*. Beograd. K6ninglich Serbische akademie, (English translation: *Canon of Insolation and the Ice Age Problem*, by Israel Program for Scientific Translation and published for the U.S. Department of Commerce and the National Science Foundation), pp. 484.
- Muller, R.A. and MacDonald, G.J., (1997a) Simultaneous presence of orbital inclination and eccentricity in the proxy climate records from Ocean Drilling Program site 806. *Geology*, v. 25, pp. 3-6.
- Muller, R.A. and MacDonald, G.J. (1997b) *Glacial Cycles and Astronomical Forcing*, *Science*, v. 277, pp. 215- 218.
- Naidu, P.D. and Malmgren, B.A. (1995) A 2200 years periodicity in the Asian monsoon system. *Geophys. Res. Lett.*, v. 22, pp. 2361-2364.
- Naik, S.S., Thamban, M., Laluraj, M., Redkar, B. L. and Chaturvedi, A. (2010) A century of climate variability in central Dronning Maud Land, East Antarctica, and its relation to southern annular mode and El-Niño – Southern-Oscillation. *J. Geophys. Res.*, v. 115, D16102, doi:10.1029/2009JD013268.
- Napier, W. M. (2001) Temporal variation of the zodiacal dust cloud. *Mont. Not. R. Astron. Soc.* v. 321, pp. 463-470.
- Napier, W. M. (2006) Evidence for cometary bombardment episodes. *Mon. Not. R. Astron. Soc.* v. 366, pp. 977-982 doi:10.1111/j.1365-2966.2005.09851.
- Neff, U, Burns S.J., Mangini A, Mudelsee, M., Fleitmann, D. and Matter, A. (2001) Strong coherence between solar variability and the monsoon in Oman between 9 and 6 kyr ago. *Nature*, v. 411, pp. 290-293.
- Nicholls, N. (1983) Predicting Indian monsoon rainfall from sea-surface temperature in the Indonesia-north Australia area. *Nature*, v. 306, pp. 576-577.
- Nicholson, S.B. (1957) *The Sunspot Cycle*. American Astronomers Report, Sky and Telescope, April, 1957.
- Nigam, R., Khare, N. and Nair, R.R. (1995) Foraminiferal evidences for 77-Year cycles of droughts in India and its possible modulation by the Gleissberg Solar cycle. *J. Coastal Res.*, v. 11, pp.1099-107.
- NOAA, Solar Geophysical Data (1984) Sunspot numbers for the period 1871-1984, World Data Center A, Washington D.C., U.S.A. (1975) and from a catalogue of Solar Geophysical Data published by NOAA, U.S.A. (1984).
- Nurmi, P., Valtonen, M.J. and Zheng J.Q (2001) Periodic variation of Oort Cloud flux and cometary impacts on the Earth and Jupiter. *Mont. Not. R. Astro. Soc.* v. 327, pp. 1367-1376.

- Okal, E. and Anderson, D.L. (1975) On the Planetary theory of the Sunspots. *Nature*, v. 253, pp.511-513.
- Paillard, D., Labeyrie, L. and Yiou, P. (1996) Macintosh program performs time series analysis. *EOS Trans AGU*, v. 77, pp. 379.
- Parthasarathy, B., Munot, A. A. and Kothawale, D. R. (1994) All-India Monthly and Seasonal Rainfall Series: 1871-1993. *Theor. Appl. Climatol.* v. 49, pp. 217-224.
- Philander, S.G.H. (1983) El-Nino Southern Oscillation. *Nature*, v. 302, pp. 296-297.
- Prell, W.L. and Kutzbach, J.E. (1992) Sensitivity of the Indian monsoon to forcing parameters and implications for its evolution. *Nature*, v. 360, pp. 647-652.
- Prell, W.L., Murray, D.W., Clemens, S.C. and Anderson, D.M. (1992) Evolution and variability of the Indian Ocean summer monsoon: Evidence from the western Arabian Sea drilling program,. In: Duncan, R.A., *et al.*, (eds.), *Synthesis of Results from Scientific Drilling in the Indian Ocean*, Geophysical Monograph 70, America Geophysical Union, Washington, D. C., pp. 447-469.
- Quade, J., Cerling, T. E. and Bowman, J. E. (1989) Development of Asian monsoon revealed by marked ecological shift during the latest Miocene in northern Pakistan. *Nature*, v. 342, pp. 163-166.
- Quinn, T. R., Tremaine, S. and Duncan, M. (1991) A three million year integration from the Earth's orbit. *Astron. J.*, v. 101, pp. 2287-2305.
- Rao, A. R. and Hameed, K. (2003) Multi-taper method of analysis of periodicities in hydrologic data. *J. Hydrology*, v. 279, pp. 125-143.
- Reid, G.C. (1987) Influence of solar variability on global sea surface temperatures. *Nature*, v. 329, pp. 142-143.
- Sadhuram, Y. (1997) Predicting monsoon rainfall and pressure indices from sea surface temperature. *Curr. Sci.* v. 72, pp. 166-168.
- Saji, N.H., Goswami, B.N., Vinayachandran, P.N. and Yamagata, T. (1999) A dipole in the tropical Indian Ocean. *Nature*, v. 401, pp. 360-369.
- Scafetta, N. (2010) Empirical evidence for a celestial origin of the climate oscillations and its implications. *J. Atmos. Solar-Terrest. Phys.*, v. 10, pp. 1-18, doi:10.1016/j.jastp.2010.04.015
- Schlitzer, R., (2001) Ocean Data View, <http://www.awi-bremerhaven.de/GEO/ODV>.
- Schulz, M. and Stattegger, K., (1997) Spectral analysis of unevenly spaced paleoclimatic time series. *Comput. Geosci.* v. 23, pp. 929-945.
- Sen Gupta, P.K. (1957) Sunspot cycle in regional rain-fall. *Weather*, v. 12, pp. 322-324.
- Shukla, K. S. (1957) The Surya Siddhanta with the Commentary of Paramesvara. Dept. of Mathematics and Astronomy, Lucknow University Research papers.
- Sikka, D.R. and Gadgil, S. (1980) On the Maximum Cloud Zone and the ITCZ over Indian, Longitudes during the Southwest monsoon. *Mon. Weather. Rev.*, v. 108, pp. 1840-1853.
- Sirocko, F. Sarnthein, M, Lange, H. and Eirlenkeuser, H. (1991) Atmospheric summer circulation and coastal upwelling in the Arabian Sea during the Holocene and the last glaciation. *Quat. Res.*, v. 36, pp.72-93.
- Sofia, S., Dunham, D.W., Dunham, J.B. and Fiala, A.D. (1983) Solar radius change between 1925 and 1979. *Nature*, v. 304, pp. 522-526.
- Solanki, S.K., Usoskin, I. G. Kromer, B. Schüssler, M. and Beer, J. (2004) Unusual activity of the Sun during recent decades compared to the previous 11,000 years. *Nature*, v. 431(7012), pp. 1084-1087.
- Surya Siddhanta, Maharishi University of Management, Vedic Literature Collection. PDF file - Mahoreg VedicFinal.qxd, by P.F. Reund – 29 July, 2002, pp. 1-55.
- Steinhilber, F., Beer, J. and Fröhlich, C. (2009) Total solar irradiance during the Holocene. *Geophys. Res. Lett.*, v. 36, pp. L19704, doi:10.1029/2009GL040142.
- Stuiver, M. and Quay, P.D. (1980) Changes in atmospheric ¹⁴C attributed to variable Sun. *Science*, v. 207, pp. 11-19.
- Thamban, M., Kawahata, H. and Rao, V.P. (2007) Indian summer monsoon variability during the Holocene as recorded in sediments of the Arabian Sea: timing and implications. *J. Oceanogr.*, V. 63, pp. 1009-1020,
- Thompson, R. (1997) Planetary Diameters in the Surya-Siddhanta. *J. Sci. Explor.* v.11, pp. 193-200, 1997
- Thomson, D.J. (1982). Spectrum estimation and harmonic analysis, *Proceed. IEEE*, v. 70, pp. 1055-1096.

- Tiwari, M., Ramesh, R., Somayajulu, B.L.K., Jull, A.J.T. and Burr, G.S. (2006) Paleomonsoon precipitation deduced from a sediment core from the equatorial Indian Ocean. *Geo-Marine Lett.*, v. 26, pp. 23-30.
- Torrence, C. and Compo, G.P. (1998) A Practical Guide to Wavelet Analysis, *Bull. Amer. Meteor. Soc.*, v.79, pp. 61-78,
- Torrence, C. and Webster, P.J. (1999) Interdecadal Changes in the ENSO–monsoon System. *J. Climate*, v. 12, pp. 2679-2690.
- Varadi, F., Runnegar, B. and Ghil, M. (2003) Successive refinements in long term integration of planetary orbits. *Astrophys. J.*, v. 592, pp. 620–630.
- von Rad U., Schaaf, M., Michels K.H., Schulz, H., Berger, W.H. and Sirocko, F. (1999) A 5000-yr record of climate change in varved sediments from the Oxygen Minimum Zone off Pakistan, northeastern Arabian Sea. *Quaternary Res.*, v. 51, pp.9–53.
- von Rad, U., Lukage, A., Berger, W.H. and Rolinski, H.D. (2006) Annual to millennial monsoonal cyclicity recorded in Holocene varved sediments from the NE Arabian Sea. *J. Geol. Soc. India*, v. 68, pp. 353-368.
- Waldauer, C., Zahka, W.J. and Pal., S. (1996) Kautilya’s Arthasastra: A neglected precursor to classical economics. *Ind. Econ. Review*, v. 31, pp. 101-108.
- Webster P. J., Magana, V.O. and Palmer, T.N. (1998) Monsoons: Processes, predictability, and the prospects for prediction. *J. Geophys. Res.*, v. 103(C7), pp. 14451–14510.
- Wood, K.D. (1972) Sunspots and planets. *Nature*, v. 240, pp. 91-93.